University of Kent at Canterbury

Hydrazine Derivatives as a Platform for Site-Specific Labelling of Peptides for *in vivo* Molecular Imaging of Disease

Charlotte Holland

A thesis submitted to the University of Kent at Canterbury for the degree of Master of Chemistry in the Faculty of Science, Technology and Medical Studies.

September 2015

Declaration

No part of this thesis has been submitted in support of an application for any other degree or qualification to the University of Kent at Canterbury or any other University or Institute of Learning.

Charlotte Holland

April 2015

Acknowledgements

I would first like to thank my supervisor, Dr Stefano Biagini for his guidance and support throughout my MSc. I would also like to thank Dr Simon Holder for his valuable input and additional support. Thank you to Jon James and all the lab technicians for their time, endless supply of equipment and excellent problem solving abilities. Thanks to Ian Ross, Mike Cole and Bernard Doolin for their technical support.

Thanks to the friends I have made within the FMG group, in particular Kate who has provided continual support and who has given up far too much of her own time to help me. I really couldn't have done it without you.

Thank you to my Dad for making it possible for me to do this.

Finally to my Mum and Mike, thank you for putting up with me when many others wouldn't, and for being there for me throughout everything.

Abstract

The 6-hydrazinonicotinyl group, known as HYNIC, is an attractive bifunctional coupling agent for preparing 99mTc-labeled peptides and proteins for medical imaging. Peptides are useful for imaging disease states such as cancer and inflammation because they take advantage of a distinct cellular target, such as a receptor, being present on the cell. Receptors are often over expressed on tumour cells. Peptides will bind to their receptors with high specificity and affinity. There is a recognized need to create well-defined polymer probes for *in vivo* and clinical PET and SPECT imaging to guide the development of new generation polymer therapeutics. In general the amount of radionuclide used in radiopharmaceuticals is small, so attaching the radionuclide to a polymer ensures that the radionuclide will be highly concentrated in the radiopharmaceutical. The number of binding sites is increased with the copolymer making it a viable choice for radiolabelling applications. The chances of successfully imaging the point of interest are therefore increased.

This thesis presents the synthesis of various HYNIC analogues that are capable of chelating technetium-99m in order to be attached to an amino acid and incorporated into a peptide sequence via solid phase peptide synthesis (SPPS) to image site-specific targets. While 6-HYNIC has been widely used, 2-HYNIC has not, and as such both of these were used in the synthesis of a number of derivatives. These derivatives were characterised by ^{1}H and ^{13}C NMR, FT-IR and melting point data was obtained for comparison with literature. A number of derivatives were successfully synthesised and purified with the aim of binding these to copolymer chains.

This work also presents the synthesis of a bifunctional copolymer (POEGMA-co-PAMA) which is biocompatible and can be attached to a HYNIC group and subsequently a peptide. This copolymer was synthesised using a controlled living radical polymerisation technique called Reversible Addition Fragmentation chain Transfer (RAFT). This technique was chosen due to its ability to synthesise polymers with predetermined molecular weights of complex architectures whilst maintaining control over polydispersity. Copolymers of varying compositions were synthesised and analysed by GPC and NMR. This method (once optimised) would allow for the copolymer to be labelled with technetium-99 for SPECT, providing an alternative bioconjugate synthetic route.

Contents

Abbreviations

AIBN	Azobisisobutyronitrile
AMA	2-aminoethyl methacrylate hydrochloride
ATRP	atom transfer radical polymerisation
Boc	butoxycarbonyl
BFC	bifunctional chelator
c.a	carrier added
c.f	carrier free
CRP	controlled free radical polymerisation
CT	computed tomography
d	doublet
dd	doublet of doublets
DCM	dichloromethane
DMF	*N, N*-dimethylformamide
DMSO	dimethylsulphoxide
DNA	deoxyribonucleic acids
DP	degree of polymerisation
EC	electron capture
EDC	1-ethyl-3-(3-dimethylaminopropyl)carbodiimide
EDDA	ethylenediamine-N,N-diacetic acid
EtOH	ethanol

GPC	gel permeation chromatography
HYNIC	6-hydrazinonicotinic acid
IgG	immunoglobin G
IR	infra red
m	medium (IR)
m	multiplet (NMR)
MHz	megahertz
MI	molecular imaging
MP	melting point
MRI	magnetic resonance imaging
n.c.a	no carrier added
NHS	N-hydroxysuccinimide
NMP	nitroxide-mediated polymerisation
NMR	nuclear magnetic resonance
OEGMA	oligo(ethylene glycol) methyl ether methacrylate
PAMA	Poly(aminoethyl methacrylate)
PEG	poly(ethylene)glycol
PET	Positron Emission Tomography
PMMA	poly(methyl methacrylate),
POEGMA	Poly(Oligo(ethylene glycol)methacrylate)
PPPDTA	2-phenylprop-2-yl phenyldithioacetate
ppm	parts per million

RAFT	reversible addition-fragmentation chain transfer polymerisation
RT	room temperature
s	singlet (NMR)
s	strong (IR)
SFRP	stable free radical polymerisation
SPECT	Single Photon Emission Computed Tomography
SPPS	solid phase peptide synthesis
t	triplet
TEA	triethylamine
THF	tetrahydrofuran
US	ultrasonography
WSC	water soluble carbodiimide
w	weak

Chapter 1- Introduction

1.1 Molecular Imaging

Modern day imaging techniques enable researchers to study molecular events in living subjects giving a wide range of data from simple planar anatomical information, to three-dimensional functional information. According to Weissleder and Mahmood, *"Molecular imaging can be broadly defined as the in vivo characterization and measurement of biologic processes at the cellular and molecular level. In contradistinction to "classical" diagnostic imaging, it sets forth to probe the molecular abnormalities that are the basis of disease rather than to image the end effects of these molecular alterations."*.[1] Molecular imaging provides *in vivo* information about proteins, genes, molecules, stem cells; thus mechanisms related to biological processes and diseases can be studied, with significant benefits, compared to *in vitro* and *ex vivo* studies. Unlike other imaging modalities such as Computed Tomography (CT), Magnetic Resonance Imaging (MRI) and Ultrasonography (US), nuclear medicine procedures are capable of mapping physiological function and metabolic activity and therefore give more specific information about the organ function and dysfunction. The mapping of the radiopharmaceutical distribution *in vivo* provides images of functional morphology of organs in a non-invasive manner and plays an important role in the diagnosis of many common diseases associated with the malfunctioning of organs in the body as well as in the detection of certain type of cancers. Radioisotope imaging uses radiation emanating from radionuclides in tracer quantity inside the subject.[2] The widespread utilization and growing demands for these techniques are directly attributable to the development and availability of a vast range of specific radiopharmaceuticals.[3-5]

The main steps in molecular imaging with radioisotopes are: (i) design of molecules that can target specific receptors; (ii) attachment of radioisotopes that emit photons (for single-photon emission computed tomography, SPECT) or positrons (for

positron emission tomography, PET) without changing the biological properties of target molecules; (iii) injection and *in vivo* imaging, by using high resolution and high sensitivity devices.[6, 7]

SPECT and PET are the two imaging modalities used in nuclear medicine. Both of these modalities offer a non-invasive method to determine the concentration of specific molecules in the human body, and are sensitive enough to visualise interactions between physiological targets and ligands.[4, 8, 9]

Molecular imaging is not however, limited to SPECT and PET. The introduction of contrast agents allow functional information to be obtained even by using Computerized Tomography (CT), Ultrasound (US), Magnetic Resonance Imaging (MRI) and the various Optical Imaging techniques. CT and MRI provide considerable anatomical information about the location and the extent of tumours as well as morphological information and potential metastases.[10, 11] US images provide information about local and regional morphology with blood flow. PET and SPECT map the location and concentration of radio-labelled compounds. As well as giving the precise location, size, shape, and viability of the tumour, PET and SPECT provide information about the molecular makeup of the tumour and its metabolic activity.[11] These imaging modalities can provide quantitative information with regards to receptor status, metabolic processes and blood flow.[12]

1.2 The Use of Radiopharmaceuticals in Nuclear Medicine

1.2.1 Radiolabelling

The application of radiolabelled peptides, peptide-hormones and proteins for diagnostic imaging and radiotherapy of cancers is a major aspect of nuclear medicine.[13, 14] Radiolabelling is the chemical reaction during which a radionuclide is incorporated into the desired molecule. A radionuclide is an isotope that undergoes radioactive decay; any element with an excess of either neutrons or protons in the nucleus is unstable and tends toward radioactive decay, with an emission of energy that can be measured with a detector. The processes of radioactive decay include beta particle emission, electron capture, isomeric transition, and positron emission. These radiolabelled compounds, known as radiopharmaceuticals, are used in low concentrations and, as such, have minimal pharmacological effect.[15] Among all the radionuclides being produced around the world, only a few combine the favourable characteristics of physical decay with desirable biological characteristics to become a useful medical radioisotope for molecular imaging.[16]

Currently there are over a hundred radiopharmaceuticals, developed using either reactor or cyclotron produced radioisotopes, which are used for the diagnosis of several common diseases and the therapy of a few selected diseases, including cancer.[3] Currently in nuclear medicine, almost 95% of radiopharmaceuticals are used for diagnostic purposes, while only 5% are used for therapeutic purposes.[15] This work focuses on the use of radiopharmaceuticals for molecular imaging and as such only these will be discussed in detail, however, it is worth noting that the same radiolabelling techniques used for imaging can be used for radiotherapy too.[17, 18]

There are several methods for radiolabelling including: isotope exchange; introduction of a foreign label; labelling with a bifunctional chelating agent (BFCA); biosynthesis; recoil labelling; and excitation labelling.[15] Two of the more popular strategies for radiolabelling involve incorporating the radiotracer into the

biomolecule, and using a bifunctional chelator (BFC) to attach the radiotracer.[19] Molecular imaging with radionuclides relies to a large extent on the formation of bioconjugates with metallic radionuclides using BFCs, which are molecules that bind covalently to the targeting molecule and chelate the radiometal, thus coupling the metal indirectly to the targeting molecule.[20, 21]

1.2.2 Properties of Radiopharmaceuticals

Radiopharmaceuticals must have a number of desirable and interrelated properties in order to be successful. They will have short effective half-lives (no longer than the time necessary to complete the study)[15] and favourable decay in order to keep the dose to the patient as low as possible. Also, the daughter nuclei should not present any additional radiological hazard. Radionuclides which decay by γ-ray emission are preferable for use in diagnostic radiopharmaceuticals as α and β particles cause more radiation damage to the tissue. For therapy however, α and β emitters are useful as they provide effective radiation damage to abnormal cells.[15] Furthermore, the metal complex (if used) must be thermodynamically stable to give high yields during production and specific activity of 100% is preferable. The radiopharmaceutical must be kinetically stable in order to remain intact long enough *in vivo* to locate the target, and it must have high affinity for its target.[22] Lipophilicity, size and total charge are some factors that have an effect on biodistribution.[23] Lipophilic compounds may diffuse across membranes like the blood/brain barrier, while the charge may help them accumulate inside the target tissue. Hydrophilic compounds tend to show rapid renal excretion. Lipophilic compounds tend to be excreted slowly via the gut. The size of the compound affects the diffusion rate.[24]

Target-specific radiopharmaceuticals consist of a moiety, such as an antibody, peptide or low molecular-weight ligand which is linked to an appropriate radionuclide.[9] Ideally these radiopharmaceuticals are designed to locate cancerous

tumours, even if their location in the body is unknown, while producing minimal radiation damage to normal tissues.[25]

The radiolabelling of amino acids and progressing from this, peptides, has been the natural progression of targeted radiopharmaceuticals over the last three decades.[26] The small compounds often possess higher target-to-background ratios and faster blood clearance than the previously favoured proteins and monoclonal antibodies.[27] Target-specific delivery of radioactive peptides, both for molecular imaging and therapy, is increasingly considered a promising strategy,[9] and peptide-based radiopharmaceuticals represent by far the largest group of tumour-targeted imaging agents currently in use.[28]

Well established solid-phase peptide synthesis allows reproducible preparation of a variety of peptides with accurate chemical structures, which can be modulated to optimize affinity and specificity for the target, metabolic stability and pharmacokinetics.[4] Peptides are useful for imaging disease states such as cancer and inflammation because they take advantage of a distinct cellular target, such as a receptor, being present on the cell. Peptides will bind to their receptors with high specificity and affinity.[29] Another advantage of peptides is their tolerance towards the modifications necessary for their labelling with different radionuclides.

For radiometallation, for example, the most explored approach makes use of a BFC that coordinates the metal and presents an adequate functionality for the coupling of the targeting peptide.[9, 21]

1.2.3 Bifunctional Chelating Agents

If radiometals are used as the radiation source, the labelling reaction is often performed through chelation.[28] The majority of diagnostic radiopharmaceuticals currently available in nuclear medicine use radiometal complexes or target-specific biomolecules labelled with metallic radionuclides.[21, 28] The biomolecules are generally derivatised with a suitable metal chelating group that provides stable

chelation of the radiometal. In general, a radiopharmaceutical containing a bifunctional chelating agent (BFCA) consists of the following parts: a targeting molecule, a bifunctional chelator (BFC), a radionuclide, and a linker.[21, 30] The targeting molecule is a carrier of the radionuclide to the receptor site *in vivo*. The radionuclide serves as the radiation source. The BFC, covalently attached to the targeting molecule, functions as the coordinator of the radionuclide. The linker, although not always necessary, acts as a spacer residue, which separates the targeting molecule from the chelating agent. The BFCA is covalently attached to functional groups which are naturally present in the peptide or have been introduced synthetically.[31]

The choice of BFC is determined by the nature and oxidation state of the radiometal; different radiometals require BFCs with different donor atoms and chelator structures.[21] The ideal BFCA should (i) coordinate a metal ion with a high yield, (ii) form metal complexes with both high thermodynamic stability and *in vivo* kinetic inertness to minimise toxicity, (iii) be produced quickly with an excellent overall yield.[32]

Hydrazine derivatives, such as 6-hydrazinopyridine-3-carboxylic acid (HYNIC), have been used routinely as BFCAs in nuclear medicine to label peptides and other biomolecules with technetium-99m for SPECT.[33] HYNIC has also been used for labelling peptides and other biomolecules with fluorine-18 for PET.[34, 35] HYNIC is an attractive BFC because of its monodenticity that allows for a variety of different coligands leading to different biodistributions.[36] Tricine and glucoheptonate are examples of coligands which allow easy modification of hydrophilicity and pharmacokinetics of technetium-99m labelled biomolecules.[21] In addition, high specific activity is obtainable using HYNIC as a chelating agent.[33, 37, 38]

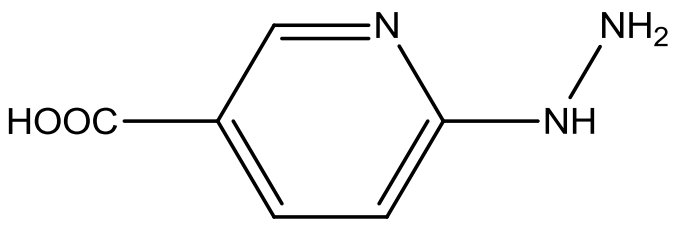

Figure 1.1: Structure of 6-HYNIC.

HYNIC can be attached to the peptide via the amino acid side chains or the N/C termini.[39] This is done post SPPS using standard conjugation techniques. Conjugation is usually via a primary amine or cystine 'handle' placed at the end of the peptide. The advantages are that a number of conjugation methods may be performed on the same batch of peptide. However, if there is more than one primary amine or the peptide requires a disulfide bond, losses in purification can occur as more than one species will be present.[40]

1.3 Positron Emission Tomography (PET)

Positron Emission Tomography (PET) is used to monitor the concentration and movement of a positron emitting isotope in living tissue.[41] PET is a powerful, non-invasive molecular imaging technique which offers picomolar sensitivity and provides functional information on physiological, biochemical and pharmacological processes in living subjects.[42] PET requires a tracer that is labelled with a positron-emitting radionuclide which can be quantified *in vivo* by the detection of the gamma rays formed as a result of the annihilation of the positrons emitted.[42]

A positron is annihilated in a distance of 1–4mm from each emission point and two opposite travelling photons are produced. The detector needs to be able to simultaneously detect those two photons, and a reconstruction algorithm is necessary to obtain the three-dimensional distribution for radiopharmaceuticals concentration. The collision of an emitted positron with a nearby electron produces two gamma rays that are separated by 180°. Two scintillation detectors that are separated by 180° transmit a coincident signal when they are achieved simultaneously. The photon energy that is absorbed by the detectors is re-emitted as visible light and detected by photomultiplier tubes. The light signal is converted into an electrical current, which is proportional to the incident photon energy. The registered events are reconstructed into a three dimensional image representing the spatial distribution of the radioactive source in the studied subject.[6, 43]

PET offers significantly improved spatial resolution and sensitivity (by 2-3 orders of magnitude) when compared with SPECT[28], and allows the performance of tomographic dynamic studies, something that is not possible with clinical SPECT equipment (with the exception of a few prototypes) [6, 44] In addition, the natural occurrence of PET isotopes in biologically active molecules provides for a less challenging task of synthesizing physiologically useful tracers in PET.[45] The main limitation of PET, when compared to SPECT, is the use of short-life isotopes **(see table 1.1)**, which increases overall cost, as well as the number of applications that can be imaged with PET isotopes.[6] Nevertheless, the short half-lives of radionuclides

used in PET effectively allow for increased detection sensitivity over a given period of time. This is because short-life isotopes can be injected in higher activities to the patient without posing any additional radiation damage to the patient (since overall accumulation over time remains the same) thus generating increased detectable radiation over a shorter time.[45] The combination of high resolution and sensitivity and the ability to carry out dynamic tomographic studies leads to a number of dedicated PET scanners.

1.3.1 PET Radionuclides

A PET radiopharmaceutical consists of two components; a molecular structure (vehicle, ligand) and a positron emitting radionuclide.[46] A linker may also be necessary to form a stable connection between the two components. The molecular structure component defines pharmacokinetics and pharmacodynamics; the biological characteristics and biochemical interactions within the living organism. These molecules must provide a high degree of specificity and selectivity towards the target site. The positron emitting radionuclide provides a detectable signal enabling coincidence measurements of annihilation radiation within a PET scanner.[47]

The choice of the PET radionuclide is imposed by its physical and chemical characteristics, availability, and the timescale of the studied biological process.[42] Positron emission is exclusively a property of neutron deficient nuclides.[48]

The choice of a radionuclide could depend on its physical half-life, which should not only allow the chemical incorporation (radiolabelling reaction) of the radionuclide into the target compound, but also match the biological half-life of a corresponding tracer in order to obtain good target to background ratio and avoid unnecessary irradiation.[21, 48]

If the tracers need to be transported from the radiolabelling sites to imaging sites, or if a relatively lengthy labelling procedure is required, it may not be possible to use short lived isotopes such as carbon-11. Due to the very short half-life of oxygen-15

and nitrogen-14 **(see table 1.1)**, the tracers prepared are usually only in the chemical forms produced in a cyclotron target, or other derivatives that were obtained by instant high yield reactions.[42] Other factors for isotope selection may include the conditions for radiolabelling, specific activity, and radionuclide production.[49]

Specific activity is important in the preparation of radioisotopes, particularly in PET where the radionuclide is incorporated into a radiotracer which is used to probe some physiological process in which very small amounts of the biomolecule are being used.[50] PET is essentially a tracer method and the goal is to probe physiological processes without disturbing the process. If the amount of radiotracer is very small in comparison to the amount of the native compound or its competitor, then the process will be minimally disturbed.[51] Specific activity is normally expressed in terms of the amount of radioactivity per mole of compound.

The positron-emitting radionuclides must be made in the targets, and then converted to a precursor, either in the target or immediately after exiting the target. The precursor is then converted into the molecule of interest.[50]

There are four positron-emitting radioisotopes which are used more often than others. These are fluorine-18, carbon-11, nitrogen-13 and oxygen-15. The reason that they are most commonly used is that they can be easily substituted directly onto the biomolecules. Carbon-11, nitrogen-13 and oxygen-15 are the *'elements of life'*;[50] the building blocks of the biochemicals that regulate biochemical processes.[52] Substitution of carbon-11 for carbon-12 does not significantly alter the reaction time or mechanism of a molecule. A similar situation exists for nitrogen-18 and oxygen-15. Fluorine-18 can often be substituted for a hydroxy group on a molecule or placed in a position where its presence does not significantly alter the biological behaviour of the molecule.[50]

Table 1.1: Short-lived PET radionuclides with half-lives and nuclear reaction for production.

Radionuclide	Half-life (minutes)	Nuclear Reaction
Carbon-11	20.4	^{14}N (p, α) ^{11}C
Nitrogen-13	9.96	^{16}O (p, α) ^{13}N
Oxygen-15	2.07	^{15}N (p, n) ^{15}O
Fluorine-18	109.8	^{18}O (p, n) ^{18}F

1.3.1.1 Radiolabelling with Fluorine-18

Fluorine-18 is the most commonly used radionuclide for routine diagnosis with PET.[53, 54] Fluorine-18 has a half-life of 110 minutes, low β^+ energy, and is easy to produce.[55] Fluorine-18 also decays 97% by positron emission (the other 3% is by electron-capture).[50] Therefore ^{18}F represents the ideal radionuclide for PET imaging. Due to its low positron energy it has a short positron linear range in tissue (max. 2.3mm), allowing for optimum resolution images in PET.[56] Furthermore, the relatively long half-life (in comparison, for example, to carbon-11, nitrogen-13 and oxygen-15) allows for syntheses of fluorine-18 labelled radiopharmaceuticals; transportation over reasonable distances; and imaging procedures to be extended over a few hours.

In order to make use of the desirable properties offered by fluorine-18, researchers have sought to develop radiochemical syntheses that are rapid, high yielding, chemoselective, and do not require deprotection steps. However, the production of ^{18}F-labelled tracers poses several challenges; 'true' or isotopic labelling is limited to molecules with a fluorine atom;[53] however there are no naturally occurring fluorine-containing compounds in the body and fluorine-containing biomolecules are often not suitable substrates in normal metabolic pathways as they can act as enzyme inhibitors.[57] Other radionuclides such as oxygen-15, nitrogen-13, and carbon-11 are able to give isotopic labelling because the elements carbon, nitrogen and oxygen are all common in nature. Therefore the radiolabelled tracers are indistinguishable from the stable isotope equivalent molecules. This is not the case for fluorine-18; instead fluorine-18 is most commonly used by replacing hydrogen in organic molecules.[54, 58] This significantly affects the chemical and biochemical properties of the molecule (e.g. distribution and metabolism).

Fluorine-18 is usually produced as fluorine gas ([^{18}F]F) by irradiating gas targets in the ^{20}Ne(d, α)^{18}F or ^{18}O(p, n)^{18}F reactions, or as aqueous ionic fluoride ([^{18}F]F^{-}) by irradiating enriched water targets in the ^{18}O(p, n)^{18}F reaction. The use of F_2 as a carrier gas is required for the production of [^{18}F]F.[50, 58]

There are various chemical reactions to incorporate the fluorine-18 isotope into target molecules but broadly speaking, labelling with fluorine-18 is either done by electrophilic substitution, using [^{18}F]F gas, or nucleophilic substitution, using the [^{18}F] fluoride ion.[50] Both of these methods yield unwanted radioactive and non-radioactive by-products that must be removed from the desired product by HPLC.

Fluorination via electrophilic substitution is carrier added (c.a) using [^{18}F]F gas, (which is produced using a neon target containing around 0.1% ^{19}F) where only one of the fluorine atoms in the [^{18}F]F gas produced will be incorporated into the target molecule.[59] The use of electrophilic fluorination reactions is therefore not ideal as the maximum achievable radiochemical yield is only 50%.[50] The electrophilic route also leads to low specific radioactivity due to the fact that carrier fluorine gas has to be added in order to recover the radiolabelled gas from the surface of the target walls. Specific activities typical for electrophilic fluorinations are around

0.4GBq/μmol whereas nucleophilic fluorinations yield specific activities in the range of 50-500GBq/μmol.[60]

Nucleophilic substitution is the most common route for labelling compounds with fluorine-18.[55] This method offers high specific radioactivity and can be both direct and indirect.[61, 62] The nucleophilic substitution (via S_N2 mechanism) is based on non-carrier added (n.c.a) [^{18}F] fluoride.[54] The n.c.a [^{18}F] fluoride is obtained in the irradiated target water which renders the ion poorly reactive; fluorine-18 forms hydrogen bonds which decrease its nucleophilicity. Therefore the labelling reactions take place under polar, aprotic conditions;[58] this produces highly reactive fluorine-18. Anhydrous acetonitrile, dimethylsulfoxide and dimethylformamide are commonly used solvents for labelling. Anion exchange resins are then used to separate [^{18}F] fluoride and recover oxygen-18 enriched target water. The last of the water is removed by azeotropic distillation under a stream of nitrogen and thermal drying at temperatures of between 80-110°C.[52, 63]

Fluorine-18 has been used to label many different biomolecules from small monomeric molecules to peptides, proteins, and oligonucleotides.[64-66] The reason for labelling peptides is that they are specific so will be taken up selectively in tissues due to the presence of a specific receptor for a particular peptide. In addition, the short biological half-life of many peptides matches the half-life of ^{18}F. Peptides can be easily synthesized and tailored for high biological activity and to facilitate radiolabelling.[67]

Anhydrous electrophilic [^{18}F]F is not used for labelling peptides. This is because its chemical lability is not appropriate for the mild, aqueous conditions generally required, and because its specific reactivity is too low.[68] Mild conditions are required as the high temperatures and strong bases that are used for radiofluorination destroy the peptides. Therefore, fluorine-18 labelled prosthetic groups have been developed.[69]

1.4 Single Photon Emission Computed Tomography (SPECT)

Single Photon Emission Computed Tomography (SPECT) is a widely used and highly sophisticated method of molecular imaging.[70] SPECT is a diagnostic imaging technique in which tomographs of a radionuclide distribution are generated from gamma photons detected at numerous positions about the distribution.[2] SPECT relies on emission of a single gamma photon with enough energy (>100 keV) to escape from the body and be detected. After injection of the radionuclide into the patient, these gamma photons are released from target areas. The photons are captured on a gamma camera that rotates around the patient. This gives an image of the radiopharmaceutical distribution.[43]

SPECT is based on the idea that a radiopharmaceutical is injected into the body and concentrates in an organ or structure of interest. SPECT can image endogenous ligands such as peptides, antibodies, hormones and selectins, which can be labelled with technetium (technetium-99m) or other isotopes.[6] Due to their size, those molecules diffuse slowly into tissue and have slow clearance from blood, which can be of the order of hours or even days. The half-life of the commonly used SPECT isotopes allows their imaging and makes possible imaging of slow processes such as cell division, infection and inflammatory processes and therapeutic radiopharmaceuticals. The use of long-life isotopes make SPECT affordable for a number of research institutions.[6] SPECT also has the unique ability to probe two or more molecular pathways simultaneously by detecting isotopes with different emission energies; thus different organs or functions can be monitored in the same time.[6]

SPECT is more widely used then PET, in part, because the synthesis of SPECT radiopharmaceuticals based on technetium-99m are produced in 'kit' form. The result of this is that the labelling procedure is simple and quick and can be carried out by a technician rather than a radiochemist. The technetium-99m (as pertechnetate ion) is added to a pre-prepared, sterile mixture of labelling precursors and additives. No final purification is necessary before injection into the patient.

This kit technology is not available for the fluorine-18 radiopharmaceuticals that are used in PET.[21, 71]

Another reason that SPECT is more widely used than PET is that technetium-99m is produced by generators that are present in all hospitals where SPECT is carried out, whereas fluorine-18 must be made by a cyclotron. Cyclotrons are too big and expensive for most hospitals to own, meaning fluorine-18 must often be produced in a different location to where it is used, causing problems with loss due to decay of the fluorine-18 nucleus during transit.[50]

1.4.1 SPECT Radionuclides

The ideal SPECT radionuclide should; be highly stable *in vivo*; exhibit excellent tissue penetration; have high affinity for the target structure; have specific uptake and retention in the target cells; have rapid clearance from non-targeted tissues and organs; and be easy to prepare.[28] Furthermore, SPECT radionuclides must either present; isomeric transition decay that emit gamma rays; or electron capture decay that emit x-rays and or gamma rays (in the range of 70-250keV).[72] The gamma emission must be strong enough to penetrate the body barrier and detectable by SPECT camera systems.[73] These characteristics are important so as to avoid unnecessary radiation dose burden to the patient as well as high background signals resulting in low tumour-to-background contrast.

Table 1.2: SPECT radionuclides with half-lives and mode of decay.

Radionuclide	Half-life	Mode of Decay
Technetium-99m	6.0 hours	IT (100%)
Iodine-123	13.2 hours	EC (100%)
Indium-111	2.8 days	EC (100%)
Gallium-67	3.3 days	EC (100%)

1.4.1.1 Radiolabelling with Technetium-99m

Technetium-99m is the most widely used radioisotope in diagnostic nuclear medicine, it is estimated that over 80% of the diagnostic nuclear medicine studies carried out annually are done with technetium-99m.[3, 21] The parent radionuclide molybdenum-99 can be prepared in abundant quantities by the fission of uranium-235 in a nuclear reactor with a fission yield of about 6%.[3] Technetium-99m from a $^{99}Mo^{99m}Tc$ generator is ideal for use with SPECT as it decays to technetium-99m with emission of gamma photons with an ideal energy of 140 keV.[74] These photons are emitted in high abundance. The half-life of 6 hours is long enough for extended procedure to be carried out, but short enough to minimise the radiation dose to the patient - radiation from the low concentrations used for imaging is relatively harmless.[21, 50] Technetium has no stable isotope and is a synthetic element.[75] The 'm' in the name technetium-99m stands for metastable nuclear isotope.[76] It does not change into another element upon decay. The rapid blood clearance and the fast tumour accumulation of small peptides allow for the use of shorter-lived radionuclides such as technetium-99m.[36 77] In routine medical practice, due to its ideal properties for SPECT and the widespread use of this imaging technique, technetium-99m is still the radionuclide of choice.

Despite the rise of PET and the growing availability of fluorine-18 as a radiolabel for PET, most widely used radiopharmaceuticals are labelled with technetium-99m.[38]

Labelling biomolecules with technetium-99m using HYNIC as the chelator differs from other BFCs, as technetium binds to the hydrazino moiety forming a Tc-N bond.[21, 78] To stabilise the molecule, co-ligands are required. Babich and Fischman first reported that the nature of the co-ligand has a significant influence on the biodistribution of the ^{99m}Tc-complex.[79] Since then, a number of co-ligands have been described, among them tricine, aminocarboxylates, and ternary ligand systems using tricine/triphenylphosphines and tricine/pyridines as co-ligands.[80]

1.5 References

1. R. Weissleder and U. Mahmood, *Radiology*, 2001, 219, 316-333.

2. M. N. Wernick and J. N. Aarsvold, *Emission Tomography: The Fundamentals of PET and SPECT*, Elsevier Science, 2004.

3. Radiopharmaceuticals: Production and Availability, *51st International Atomic Energy Agency General Conference*, Vienna, 2007.

4. S. Lee, J. Xie and X. Chen, *Biochemistry*, 2010, 49, 1364-1376.

5. M. M. Khalil, J. L. Tremoleda, T. B. Bayomy and W. Gsell, *International Journal of Molecular Imaging*, 2011, 2011.

6. G. Loudos, G. C. Kagadis and D. Psimadas, *European Journal of Radiology*, 2011, 78, 287-295.

7. M. T. Munley, G. C. Kagadis, K. P. McGee, A. S. Kirov, S. Jang, S. Mutic, R. Jeraj, L. Xing and J. D. Bourland, *Medical physics*, 2013, 40, 101501.

8. Y. Zhou, S. Chakraborty and S. Liu, *Theranostics*, 2011, 1, 58-82.

9. J. D. G. Correia, A. Paulo, P. D. Raposinho and I. Santos, *Dalton Transactions*, 2011, 40, 6144-6167.

10. G. Antoch and A. Bockisch, *European Journal of Nuclear Medicine and Molecular Imaging*, 2009, 36, 113-120.

11. D. J. Yang, T. Inoue and E. E. Kim, in *Clinical PET and PET/CT*, Springer, 2013, pp. 59-77.

12. W. A. Weber, N. Avril and M. Schwaiger, *Strahlentherapie und Onkologie*, 1999, 175, 356-372.

13. M. Fani and H. Maecke, *European Journal of Nuclear Medicine and Molecular Imaging*, 2012, 39, 11-30.

14. S. Richter and F. Wuest, *Molecules*, 2014, 19, 20536-20556.

15. G. Saha, in *Fundamentals of Nuclear Pharmacy*, Springer New York, 2010, pp. 83-113.

16. D. Schlyer, *Annals Academy Of Medicine Singapore*, 2004, 33, 146-154.

17. R. E. Weiner and M. L. Thakur, *BioDrugs*, 2005, 19, 145-163.

18. E. Bombardieri, J. Buscombe, G. Lucignani and O. Schober, *Advances in Nuclear Oncology:: Diagnosis and Therapy*, CRC Press, 2007.

19. D. Yang, I. H. Shih and E. E. Kim, in *Clinical PET and PET/CT*, eds. E. E. Kim, M.-C. Lee, T. Inoue and W.-H. Wong, Springer New York, 2013, pp. 79-84.

20. L. K. Meszaros, A. Dose, S. C. G. Biagini and P. J. Blower, *Dalton Transactions*, 2011, 40, 6260-6267.

21. S. Liu, *Advanced Drug Delivery Reviews*, 2008, 60, 1347-1370.

22. C. A. Boswell and M. W. Brechbiel, *Nuclear Medicine and Biology*, 2007, 34, 757-778.

23. M. Tabrizi, G. G. Bornstein and H. Suria, *The AAPS Journal*, 2010, 12, 33-43.

24. E. E. Kim, D. Lee and R. P. Baum, *Handbook of Nuclear Medicine and Molecular Imaging: Principles and Clinical Applications*, World Scientific, 2012.

25. W. A. Volkert and T. J. Hoffman, *Chemical Reviews*, 1999, 99, 2269-2292.

26. M. Fani, H. R. Maecke and S. M. Okarvi, *Theranostics*, 2012, 2, 481-501.

27. R. Alberto, *Contrast Agents III*, 2005, 1-44.

28. C. Müller and R. Schibli, in *Molecular Imaging in Oncology*, Springer, 2013, pp. 65-105.

29. S. Lee, J. Xie and X. Chen, *Chemical Reviews*, 2010, 110, 3087-3111.

30. S. Liu, *Bifunctional chelant for attaching diagnostic metals and therpeutic isotopes to target specific biomolecules; heavy metal detoxification*, US6565828 B2, 2003.

31. C. Lozza, I. Navarro-Teulon, A. Pèlegrin, J.-P. Pouget and E. Vivès, *Frontiers in Oncology*, 2013, 3, 247.

32. E. Benoist, Y. Coulais, M. Almant, J. Kovensky, V. Moreau, D. Lesur, M. Artigau, C. Picard, C. Galaup and S. G. Gouin, *Carbohydrate Research*, 2011, 346, 26-34.

33. J. W. Babich, H. Solomon, M. C. Pike, D. Kroon, W. Graham, M. J. Abrams, R. G. Tompkins, R. H. Rubin and A. J. Fischman, *Journal of Nuclear Medicine*, 1993, 34, 1964-1974.

34. H. J. Rennen, P. Laverman, J. E. van Eerd, W. J. Oyen, F. H. Corstens and O. C. Boerman, *Nuclear Medicine and Biology*, 2007, 34, 691-695.

35. K. Bruus-Jensen, T. Poethko, M. Schottelius, A. Hauser, M. Schwaiger and H.-J. Wester, *Nuclear Medicine and Biology*, 2006, 33, 173-183.

36. M. Gandomkar, R. Najafi, M. Shafiei, M. Mazidi and S. E. S. Ebrahimi, *Nuclear Medicine and Biology*, 2007, 34, 651-657.

37. R. C. King, M. B.-U. Surfraz, S. C. G. Biagini, P. J. Blower and S. J. Mather, *Dalton transactions (Cambridge, England : 2003)*, 2007, 4998-5007.

38. L. K. Meszaros, A. Dose, S. C. Biagini and P. J. Blower, *Inorganica Chimica Acta*, 2010, 363, 1059-1069.

39. H. Jiang, B. B. Kasten, H. Liu, S. Qi, Y. Liu, M. Tian, C. L. Barnes, H. Zhang, Z. Cheng and P. D. Benny, *Bioconjugate Chemistry*, 2012, 23, 2300-2312.

40. V. Tolmachev and S. Stone-Elander, *Biochimica et Biophysica Acta (BBA) - General Subjects*, 2010, 1800, 487-510.

41. S. S. Gambhir, *Nature Reviews Cancer*, 2002, 2, 683-693.

42. K. Serdons, A. Verbruggen and G. M. Bormans, *Methods*, 2009, 48, 104-111.

43. C. S. Levin, *European Journal of Nuclear Medicine and Molecular Imaging*, 2005, 32, S325-S345.

44. H. Zaidi, *Quantitative Analysis in Nuclear Medicine Imaging*, Springer US, 2006.

45. A. Rahmim and H. Zaidi, *Nuclear medicine communications*, 2008, 29, 193-207.

46. P. H. Elsinga, *Nuclear Medicine Review*, 2012, 15, 13-16.

47. W. Wadsak and M. Mitterhauser, *European Journal of Radiology*, 2010, 73, 461-469.

48. I. Velikyan, 2005.

49. Z. B. Li and P. S. Conti, *Advanced Drug Delivery Reviews*, 2010, 62, 1031-1051.

50. M. J. Welch and C. S. Redvanly, *Handbook of Radiopharmaceuticals: Radiochemistry and Applications*, Wiley, 2003.

51. J. L. Musachio, J. E. Flesher, U. A. Scheffel, P. Rauseo, J. Hilton, W. B. Mathews, H. T. Ravert, R. F. Dannals and J. James Frost, *Nuclear Medicine and Biology*, 2002, 29, 547-552.

52. M. Goodman, G. Kabalka, D. Longford, T. L. Collier and T. Gotsick, in *Chemists' Views of Imaging Centers*, ed. A. Emran, Springer US, 1995, pp. 347-356.

53. P. A. Schubiger and L. Lehmann, *PET Chemistry: The Driving Force in Molecular Imaging*, Springer, 2007.

54. H. Coenen, in *PET Chemistry*, Springer, 2007, pp. 15-50.

55. Y. Gu, D. Huang, Z. Liu, J. Huang and W. Zeng, *Medicinal Chemistry*, 2011, 7, 334-344.

56. J. M. Chezal, L. Rbah-Vidal, E. Billaud, P. Auzeloux, J. C. Madelmont, A. VIDAL, E. Miot-Noirault, J. Papon and A. MAISONIAL, *Labelled quinoxaline*

derivatives as multimodal radiopharmaceuticals and their precursors, US 20150079000 A1, 2013.

57. A. Strunecká, J. Patočka and P. Connett, *Journal of Applied Biomedicine*, 2004, 2, 141-150.

58. L. Cai, S. Lu and V. W. Pike, *European Journal of Organic Chemistry*, 2008, 2008, 2853-2873.

59. Fluorine-18 labeling methods: Features and possibilities of basic reactions, *Ernst Schering Research Foundation workshop*, 2006.

60. T. L. Ross and H. J. Wester, in *Handbook of Nuclear Chemistry*, eds. A. Vértes, S. Nagy, Z. Klencsár, R. Lovas and F. Rösch, Springer US, 2011, pp. 2021-2071.

61. W.-J. Kuik, I. P. Kema, A. H. Brouwers, R. Zijlma, K. D. Neumann, R. A. J. O. Dierckx, S. G. DiMagno and P. H. Elsinga, *Journal of Nuclear Medicine*, 2015, 56, 106-112.

62. L. Carroll, S. Boldon, R. Bejot, J. E. Moore, J. Declerck and V. Gouverneur, *Organic & biomolecular chemistry*, 2011, 9, 136-140.

63. H. Slader, New strategies for the introduction of 18F into peptides for imaging with Positron Emission Tomography, University of Kent, 2009.

64. W. Cai, X. Zhang, Y. Wu and X. Chen, *Journal of Nuclear Medicine*, 2006, 47, 1172-1180.

65. S. Okarvi, *European Journal of Nuclear Medicine*, 2001, 28, 929-938.

66. H. Wester and M. Schottelius, in *PET Chemistry*, Springer, 2007, pp. 79-111.

67. M. Glaser, E. Arstad, S. K. Luthra and E. G. Robins, *Journal of Labelled Compounds & Radiopharmaceuticals*, 2009, 52, 327-330.

68. V. Tolmachev and S. Stone-Elander, *Biochimica Et Biophysica Acta-General Subjects*, 2010, 1800, 487-510.

69. M. Jamous, U. Haberkorn and W. Mier, *Molecules*, 2013, 18, 3379-3409.

70. M. D. Devous, *NeuroRx*, 2005, 2, 237-249.

71. U. Mazzi, R. Schibli, H.-J. Pietzsch, J.-U. Künstler and H. Spies, in *Technetium-99m Pharmaceuticals*, Springer, 2007, pp. 7-58.

72. D. M. M. Mattos, M. L. Gomes, R. S. Freitas, S. Moreno, G. L. Lima-Filho, E. F. Paula, R. L. C. Jales and M. Bernardo-Filho, *Journal of Labelled Compounds and Radiopharmaceuticals*, 2001, 44, S841-S843.

73. H. J. Biersack and L. M. Freeman, *Clinical Nuclear Medicine*, Springer, 2008.

74. A. Dash, F. R. Knapp Jr and M. Pillai, *RSC Advances*, 2013, 3, 14890-14909.

75. U. Abram and R. Alberto, *Journal of the Brazilian Chemical Society*, 2006, 17, 1486-1500.

76. J. Moore, C. Stanitski and P. Jurs, *Chemistry: The Molecular Science*, Cengage Learning, 2007.

77. A. Mahmood and A. G. Jones, 2003.

78. R. Alberto, in *Contrast Agents III*, Springer, 2005, pp. 1-44.

79. J. W. Babich and A. J. Fischman, *Nuclear Medicine and Biology*, 1995, 22, 25-30.

80. C. Decristoforo and S. J. Mather, *Nuclear Medicine and Biology*, 1999, 26, 389-396.

81. M. J. Abrams, M. Juweid, C. I. Tenkate, D. A. Schwartz, M. M. Hauser, F. E. Gaul, A. J. Fuccello, R. H. Rubin, H. W. Strauss and A. J. Fischman, *Journal of Nuclear Medicine*, 1990, 31, 2022-2028.

82. S. Rajabifar, M. Akhlaghi, A. R. Jalilian, F. Bolourinovin, B. Maashkar, M. Talebimehrdar and M. Ghafouri, *Nukleonika*, 2009, 54, 279-284.

83. Y. Zhou, S. Chakraborty and S. Liu, *Theranostics*, 2011, 1, 58.

84. A. Purohit, S. Liu, D. Casebier and D. S. Edwards, *Bioconjugate Chemistry*, 2003, 14, 720-727.

85. M. B. U. Surfraz, R. King, S. J. Mather, S. C. G. Biagini and P. J. Blower, *Journal of Medicinal Chemistry*, 2007, 50, 1418-1422.

86. Y.-S. Kim, Z. He, W.-Y. Hsieh and S. Liu, *Bioconjugate Chemistry*, 2006, 17, 473-484.

87. S. Liu, D. S. Edwards, R. J. Looby, A. R. Harris, M. J. Poirier, J. A. Barrett, S. J. Heminway and T. R. Carroll, *Bioconjugate Chemistry*, 1996, 7, 63-71.

88. F. Yurt Lambrecht, K. Durkan, A. Özgür, C. Gündüz, Ç. B. Avci and S. Y. Susluer, *Journal of drug targeting*, 2013, 21, 383-388.

89. V. Mäde, S. Els-Heindl and A. G. Beck-Sickinger, *Beilstein journal of organic chemistry*, 2014, 10, 1197-1212.

90. J. M. Palomo, *RSC Advances*, 2014, 4, 32658-32672.

91. M. Fani, H. Maecke and S. Okarvi, *Theranostics*, 2012, 2, 481.

92. S. Liu, W.-Y. Hsieh, Y.-S. Kim and S. I. Mohammed, *Bioconjugate Chemistry*, 2005, 16, 1580-1588.

Chapter 2 - Syntheses of HYNIC Analogues

2.1 Introduction to HYNIC

The first example using HYNIC (6-hydrazinonicotinic acid) as a bifunctional chelating agent (BFCA) for the synthesis of a radiopharmaceutical was the labelling of human polyclonal immunoglobin G (IgG) with technetium-99m and indium-111 by Abrams and co-workers in 1990.[1] Since then, HYNIC or 6-hydrazinonicotinic acid has been used routinely as a bifunctional chelating agent in nuclear medicine to label peptides and other biomolecules with technetium-99m for SPECT (single photon emission computed tomography).[2-4] It has also been used for labelling peptides and other biomolecules with fluorine-18 for PET (positron emission tomography).[5]

For SPECT imaging a complex is formed between a bifunctional chelator (BFC) and the radionuclide which then binds covalently to a specific target, for example, a cancer receptor. HYNIC has been one of the most effective BFC's used for this purpose.[6, 7]

HYNIC is a well-established bifunctional technetium-binding ligand used to synthesise technetium-99m-radiolabelled bioconjugates.[8] HYNIC binds to technetium-99m via the hydrazino group to form a Tc-N bond in high yield.[9] Conventionally, HYNIC is coupled non-site-specifically with amine groups of lysine side chains and N-terminal residues using an activated ester form of Boc-protected HYNIC, such as the Boc-HYNIC-n-hydroxysuccinimide ester. This strategy cannot discriminate between different lysine residues and gives non-site-specific labelling.[10]

Alternatively, an active ester derivative of HYNIC can be used to radiolabel antibodies or it can be attached to an amino acid and incorporated into a peptide sequence *via* solid phase peptide synthesis (SPPS) to image site-specific targets.

Since HYNIC serves as a monodentate or bidentate ligand, a coligand is necessary to complete the coordination sphere of the technetium core.[11] **(see figure 2.1)**. The most commonly used co-ligands for HYNIC are tricine and ethylenediamine-N,N-diacetic acid (EDDA)[12, 13] **(see figure 2.2)**. The requirement for co-ligands leads to not only a high degree of versatility in design and application of this bifunctional chelating system, but also a high degree of uncertainty in the structure of the coordination sphere and in how to optimise it to produce radiopharmaceuticals with the best convenience and efficiency of labelling, structural homogeneity, *in vivo* stability and targeting properties.[9] Developments and enhancements to improve its efficacy and versatility include designs to allow site specificity, availability of amino acid building blocks, improved protecting groups and a varied choice of co-ligands.[14]

1 **2**

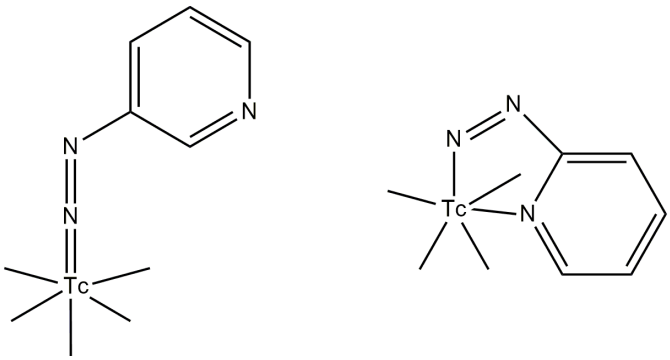

Figure 2.1: Structures of ^{99m}Tc-HYNIC-peptide complexes showing **(1)** monodentate and **(2)** bidentate binding modes.[9]

1 **2**

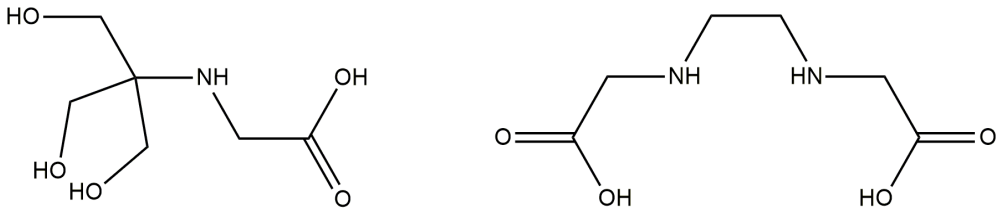

Figure 2.2: (1) Tricine and **(2)** EDDA.[9]

Technetium-99m is currently the most widely used radioisotope for SPECT due to its easy availability and half-life of 6 hours, resulting in relatively low radioactivity emission to the patient.[15]

2.2 Aims and Objectives

The 6-hydrazinonicotinyl group, known as HYNIC, is an attractive bifunctional coupling agent for preparing ^{99m}Tc-labeled peptides and proteins for medical imaging.

The aim of this chapter is to synthesise HYNIC analogues that are capable of chelating technetium-99m which can then be attached to an amino acid and incorporated into a peptide sequence *via* solid phase peptide synthesis (SPPS) to image site-specific targets.

Solid Phase Peptide Synthesis (SPPS) is a technique for forming peptides that can be readily automated with a robotic synthesiser.[16] SPPS works by sequentially attaching an amino acid to a growing peptide chain supported on a polystyrene resin bead.[17]

Peptides are specific so they will be taken up selectively in tissues due to the presence of a specific receptor for a particular peptide. Peptides are useful for imaging disease states such as cancer and inflammation because they take advantage of a distinct cellular target, such as a receptor, being present on the cell.[18] Receptors are often over expressed on tumour cells. Peptides will bind to their receptors with high specificity and affinity.[19]

Before the active ester derivative of HYNIC can be incorporated into a peptide, the hydrazine group must be protected. This is achieved with a Boc (butoxycarbonyl) group, which prevents the highly nucleophilic hydrazine group undergoing unwanted side reactions.

Active esters are improved conjugation reagents which are prepared by the action of a dehydrating agent (D) on a ligand containing a free carboxylic acid and a hydroxyl on a potential leaving group (L) **(see scheme 2.1)**. The active ester reacts cleanly with deprotonated primary amines to form a very stable amide bond **(see scheme**

2.2). The reaction can be carried out in aqueous conditions or using organic solvents.[20]

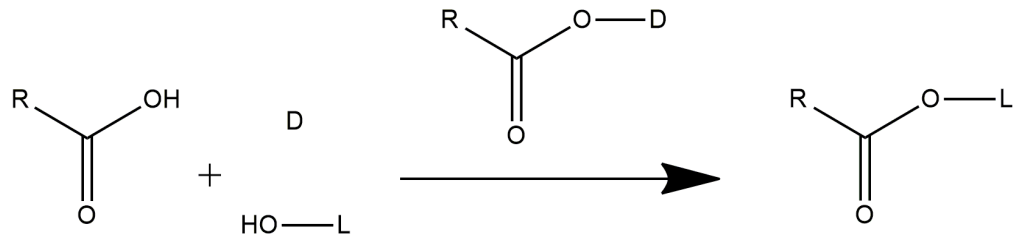

Scheme 2.1: General scheme for the preparation of an active ester.

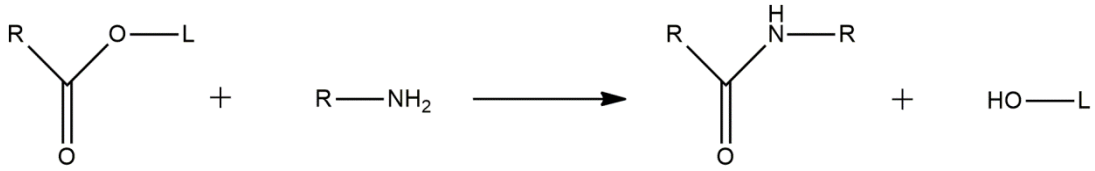

Scheme 2.2: Reaction of an active ester with a primary amine.

The active ester of Boc-HYNIC is synthesised in this chapter for the subsequent conjugation with an amino acid to be incorporated into a peptide sequence *via* solid phase peptide synthesis (SPPS). Adding HYNIC to the peptide during solid phase synthesis allows for greater flexibility and control over the position of the HYNIC within the peptide.[20]

2.3 Experimental Section

2.3.1 Materials

Anhydrous sodium sulfate, 6-chloronicotinic acid (99%), N-hydroxysuccinimide (98%), water soluble carbodiimide hydrochloride (WSC.HCl) (99%) and hydrazine hydrate (80%, hydrazine 51%) were purchased from Acros Organics (Fisher). 2-chloronicotinic acid (99%) was purchased from Alfa Aesar. Concentrated hydrochloric acid (32%), ammonium chloride, absolute ethanol (analytical reagent grade), ethyl acetate (analytical reagent grade), diethyl ether (analytical reagent grade) and dimethylformamide were bought from Fisher Scientific. Triethylamine (99%) and di-tert-butyl dicarbonate (99%) were purchased from Sigma Aldrich. Dimethyl sulphoxide-d_6 (99.9%) was purchased from Goss Scientific Instruments Ltd. All chemicals and solvents were used without further purification.

2.3.2 Instrumentation and Analysis

^{1}H and ^{13}C NMR: ^{1}H and ^{13}C nuclear magnetic resonance (NMR) spectra were recorded using a JEOL ECS-400 spectrometer at 30°C from solutions in $CDCl_3$.

IR: The IR spectra were recorded using an IR Affinity-1 Fourier Transform Infrared Spectrophotometer Shimadzu. A small amount of dry solid (about 25-50mg) was placed on the sample disc and analysed directly.

MP: The melting points were recorded using a STUART SMP10 melting point model. The samples were heated at 5 degrees per minute to reach plateau 20 degrees

below approximate melting point and then the sample was ramped at 2 degrees per minute to observe the accurate melting point.

2.3.3 Syntheses of HYNIC Analogues

2.3.3.1 Synthesis of 6-hydrazinonicotinic acid (6-hydrazinopyridine-3-carboxylic acid); 'HYNIC'[1]

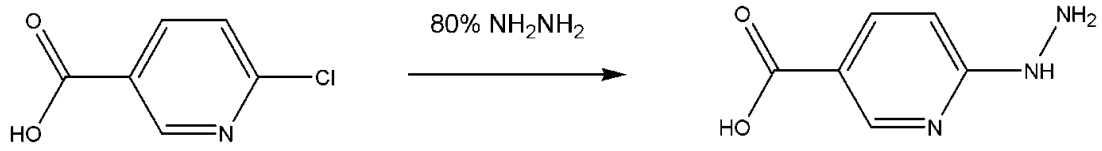

Scheme 2.3: Reaction scheme for the preparation of 6-hydrazinopyridine-3-carboxylic acid.

6-Chloronicotinic acid (1.02 g; 6.35 mmol) was added to 80% hydrazine hydrate (4.50 ml; 116.28 mmol) and placed in a 100°C oil bath for 4 hours. The homogeneous reaction mixture was cooled to room temperature and concentrated to dryness to give a light yellow solid. The solid was dissolved in water and on acidification to pH 5.5 with concentrated hydrochloric acid, a precipitate was formed. The precipitate was isolated by filtration and the solid was washed with 95% ethanol (100 cm^3) and ether (100 cm^3) and dried in a vacuum oven to give 0.72 g of 6-hydrazinopyridine-3-carboxylic acid as a yellow solid.

Yield: 0.72 g, 4.70 mmol, 74% (lit 77%), **M.P.** 285-288°C (lit 292-293°C)

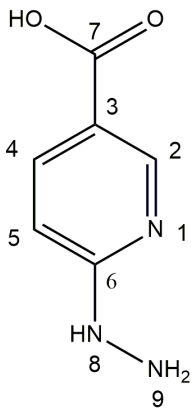

^{1}H-NMR from literature[1] (270 MHz; $(CD_3)_2SO$): δ 6.69 (1H, d, *J* = 8.0 Hz), 7.84 (1H, dd, *J* = 2.4, 8.8 Hz), 8.51 (1H, d, *J* = 2.4 Hz).

^{1}H-NMR (399.78 MHz; $(CD_3)_2SO$): δ 6.94 (1H, d, *J* = 8.4 Hz, 5-H), 8.07 (1H, dd, *J* = 2.0, 8.8 Hz, 4-H), 8.63 (1H, d, *J* = 2.0 Hz, 2-H). OH proton was observed as a broad singlet at 10.24 ppm. 8-H and 9-H were observed as a broad signal between 2.5 ppm and 4.5 ppm.

^{13}C-NMR (100.53 MHz; $(CD3)_2SO$): δ 108.9 (C-5), 118.6 (C-3), 138.9 (C-4), 148.0 (C-2), 158.1 (C-6), 166.0 (C-7).

IR: ν_{max}/cm^{-1} 3350 (m, N-H stretch, secondary amine) 3223 (m, N-H_2 stretch, primary amine), 2691 (m, O-H stretch, carboxylic acid), 1663 (s, C=O stretch, carboxylic acid).

2.3.3.2 Synthesis of 6-BOC-hydrazinopyridine-3-carboxylic acid; 'BOC-HYNIC'[1]

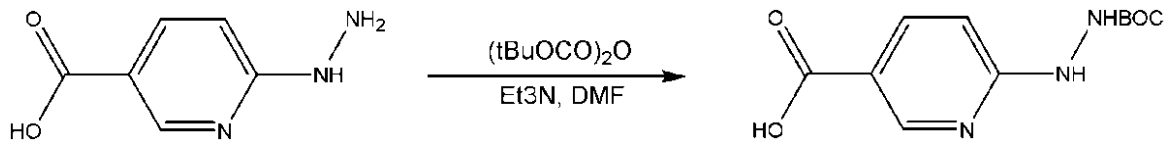

Scheme 2.4: Reaction sequence for the preparation of 6-BOC-hydrazinopyridine-3-carboxylic acid.

To a solution of 6-hydrazinopyridine-3-carboxylic acid (0.50 g; 3.26 mmol) and triethylamine (0.91 ml; 6.52 mmol) in DMF (8 ml) was added di-tert-buty dicarbonate (1.07 g; 4.89 mmol). The reaction mixture became homogeneous over 1 hour and stirring was continued for 16 hours at room temperature. The reaction mixture was concentrated to remove as much as DMF as possible under reduced pressure to give a yellow solid. The resulting yellow paste was dissolved in a minimum amount of ethyl acetate and shaken in a separating funnel with 8 aliquots of saturated ammonium chloride solution (100 cm^3 each). The organic layer was dried with sodium sulfate and vacuum filtered to give a clear yellow solution. This was concentrated to dryness and dried in a vacuum oven (60°C, 24 hours) to yield a yellow solid which was used without further purification.

Yield: 0.81 g, 3.20 mmol, 98% (lit 94%), **M.P.** 142-145°C (literature not reported)

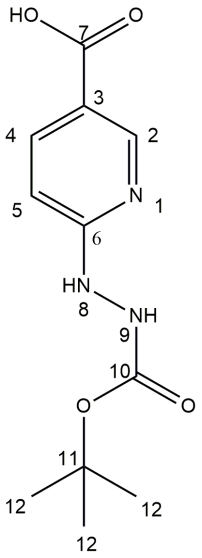

^{1}H-NMR from literature[1] (270 MHz; $(CD_3)_2SO$): δ 1.40 (9H, s) 6.52 (1H, d, *J* = 8.8 Hz), 7.97 (1H, dd, *J* = 2.4, 8.8 Hz), 8.58 (1H, d, *J* = 2.4 Hz).

^{1}H-NMR (399.78 MHz; $(CD_3)_2SO$): δ 1.34 (9H, s, 12-H) 6.58 (1H, d, *J* = 8.4 Hz, 5-H), 7.92 (1H, dd, *J* = 2.0, 8.0 Hz, 4-H), 8.53 (1H, d, *J* = 2.0 Hz, 2-H), 8.87 (1H, s, 9-H) 8.96 (1H, s, 8-H) OH proton was not observed.

^{13}C-NMR (100.53 MHz; $(CD_3)_2SO$): δ 28.6 (C-12), 79.7 (C-11), 105.0 (C-5), 116.8 (C-3), 138.9 (C-4), 150.9 (C-2), 156.4 (C-10), 162.8 (C-6), 166.9 (C-7).

IR: ν_{max}/cm^{-1} 3244 (m, N-H stretch, secondary amine) 2978 (m, C-H stretch), 1701, 1683 (s, C=O stretch, carboxylic acid), 1240, 1205, 1153 (s, C-O stretch, ester).

2.3.3.3 Synthesis of succinimidyl 6-BOC-hydrazinopyridine-3-carboxylic acid; 'NHS-HYNIC-BOC'[1]

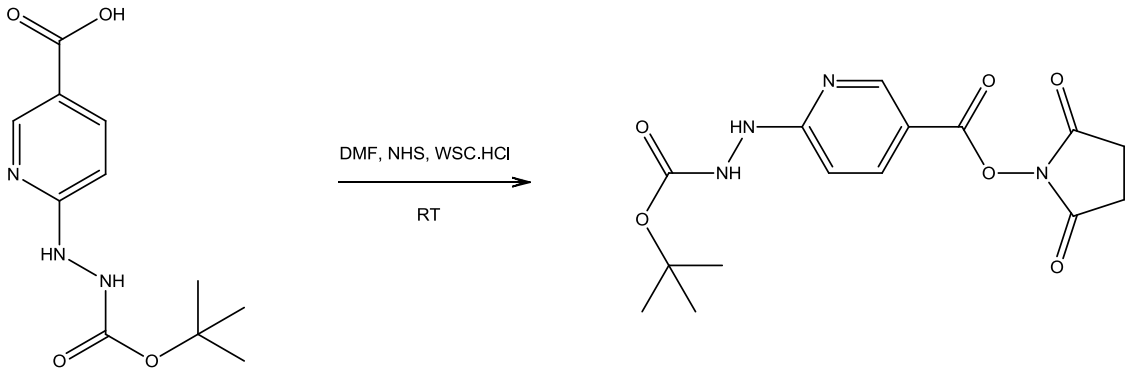

Scheme 2.5: Reaction sequence for the preparation of Succinimidyl 6-BOC-hydrazinopyridine-3-carboxylic acid.

To a solution of 6-BOC-hydrazinopyridine-3-carboxylic acid (0.10 g; 0.39 mmol) and N-hydroxysuccinimide (0.05 g; 0.39 mmol) in DMF (4 ml) was added a solution of WSC.HCl (0.08 g; 0.39 mmol) in DMF (2 ml). The reaction mixture became cloudy after 1 hour and stirring was continued for 16 hours at room temperature. The reaction mixture was concentrated to remove as much as DMF as possible under reduced pressure to give a yellow solid. The resulting yellow paste was dissolved in a minimum amount of ethyl acetate and shaken in a separating funnel with 8 aliquots of saturated ammonium chloride solution (100 cm^3 each). The organic layer was dried with sodium sulfate and vacuum filtered to give a clear yellow solution. This was concentrated to dryness and dried in a vacuum oven (60°C, 24 hours) to yield a yellow solid which was used without further purification. The eluate was concentrated to dryness to give 0.09 g of a yellow solid, which was recrystallized from ethyl acetate/hexanes.

Yield: 0.09g, 0.25mmol, 62% (lit 60%), **M.P.** 166-167°C (lit 169.5-172°C)

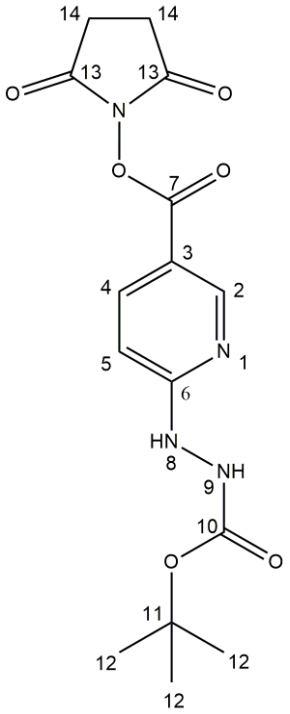

^{1}H-NMR from literature[1] (270 MHz; $(CD_3)_2SO$): δ 1.41 (9H, s), 2.87 (4H, s), 6.64 (1H, d, *J* = 8.8 Hz), 8.08 (1H, dd, *J* = 2.4, 8.8 Hz), 8.73 (1H, d, *J* = 2.4 Hz).

^{1}H-NMR (399.78 MHz; $(CD_3)_2SO$): δ 1.39 (9H, s, 12-H) 2.83 (4H, s, 14H), 6.52 (1H, d, *J* = 8.4 Hz), 7.94 (1H, dd, *J* = 2.2, 8.4 Hz), 8.58 (1H, d, *J* = 2.2 Hz), 8.94 (1H, s, 8-H), 9.27 (1H, s, 9-H).

^{13}C-NMR (100.53 MHz; $(CD_3)_2SO$): δ 24.8 (C-14), 28.6 (C-12), 80.5 (C-11), 105.0 (C-5), 112.8 (C-3), 139.4 (C-4), 150.9 (C-2), 156.4 (C-6), 162.7 (C-13), 168.9 (C-10), 170.4 (C-7).

IR: ν_{max}/cm^{-1} 3361 (m, N-H stretch, secondary amine) 2927 (m, C-H stretch), 1734, 1717 (s, C=O stretch, ester), 1647, 1601 (s, C=O stretch, amide), 1240, 1206, 1153 (s, C-O stretch, ester).

2.3.3.4 Synthesis of 2-hydrazinonicotinic acid (2-hydrazinopyridine-3-carboxylic acid); 'HYNIC'[21]

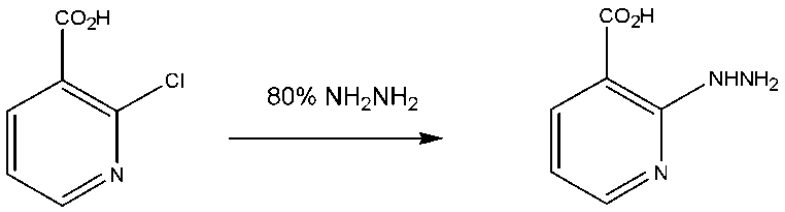

Scheme 2.6: Reaction sequence for the preparation of 2- hydrazinopyridine-3-carboxylic acid.

2-chloronicotinic acid (1.01 g, 6.44 mmol) was add to 80% hydrazine hydrate (4.60 ml; 117.98 mmol) and placed in a 100°C oil bath for 4 hours. The homogeneous reaction mixture was cooled to room temperature and concentrated to dryness under vacuum to give a yellowish solid. The solid was dissolved in water; on acidification to pH 5.0 with concentrated hydrochloric acid a precipitate was formed. The precipitate was isolated by filtration and washed with 95% ethanol ($100cm^3$) and ether ($100cm^3$) and dried in vacuum oven to give 0.50 g of 2-hydrazinopyridine-3-carboxylic acid as an orange solid.

Yield: 0.50 g, 51% (lit 57%), **M.P.** 194-196°C (literature not reported)

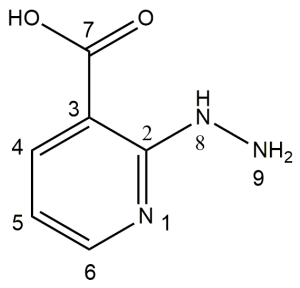

^{1}H-NMR from literature[21] (270 MHz; $(CD_3)_2SO$): δ 6.85 (1H, dd, *J* = 5.1, 7.7 Hz, 5-H), 8.15 (1H, dd, *J* = 1.7, 7.7 Hz, 4-H), 8.30 (1H, dd, *J* = 1.7, 5.1 Hz, 6-H).

^{1}H-NMR (399.78 MHz; $(CD_3)_2SO$): δ 6.30 (1H, dd, *J* = 5.2, 7.6 Hz, 5-H), 8.04 (1H, dd, *J* = 2.0, 7.6 Hz, 4-H), 8.18 (1H, dd, *J* = 2.0, 5.2 Hz, 6-H). OH proton was observed as a broad singlet at 9.31 ppm. 8-H and 9-H were not observed.

^{13}C-NMR (100.53 MHz; $(CD_3)_2SO$): δ 109.8 (C-3), 112.3 (C-5), 140.9 (C-4), 150.8 (C-6), 159.4 (C-2), 168.7 (C-7).

IR: ν_{max}/cm^{-1} 3306 (m, N-H stretch, secondary amine) 3202 (m, N-H_2 stretch, primary amine), 2950 (m, O-H stretch, carboxylic acid), 1655 (s, C=O stretch, carboxylic acid).

2.3.3.5 Synthesis of 2-BOC-hydrazinopyridine-3-carboxylic acid; '2-BOC-HYNIC'[21]

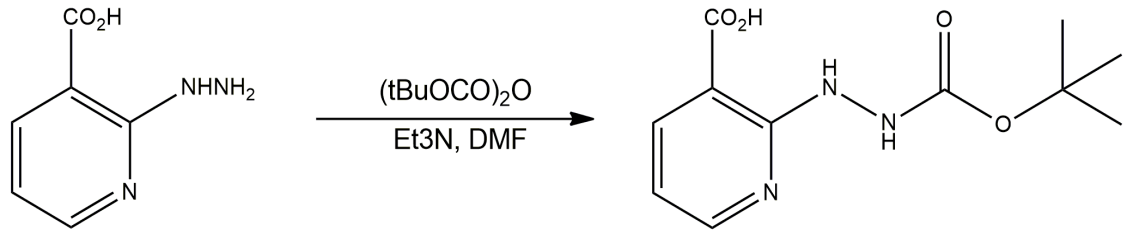

Scheme 2.7: Reaction sequence for the preparation of 2-BOC-hydrazinopyridine-3-carboxylic acid.

To a solution of 2-hydrazinopyridine-3-carboxylic acid (0.10 g; 0.65 mmol) and triethylamine (0.13 ml; 1.30 mmol) in DMF (2 ml) was added di-tert-buty dicarbonate (0.21 g; 0.98 mmol). The reaction mixture became homogeneous over 1 hour and stirring was continued for 16 hours at room temperature. The reaction mixture was concentrated to remove as much as DMF as possible under reduced pressure to give a yellow solid. The resulting yellow paste was dissolved in a minimum amount of ethyl acetate and shaken in a separating funnel with 8 aliquots of saturated ammonium chloride solution (100 cm^3 each). The organic layer was dried with sodium sulfate and vacuum filtered to give a clear yellow solution. This was concentrated to dryness and dried in a vacuum oven (60°C, 24 hours) to yield a yellow solid which was used without further purification.

Yield: 0.14 g, 0.56 mmol, 86% (lit not reported), **M.P.** 165°C (literature not reported)

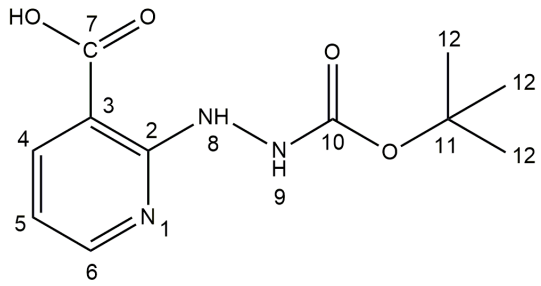

^{1}H-NMR (399.78 MHz; $(CD_3)_2SO$): δ 1.42 (9H, s, 12-H) 6.62 (1H, dd, *J* = 5.0, 7.4 Hz, 5-H), 8.04 (1H, dd, *J* = 2.0, 7.4 Hz, 4-H), 8.54 (1H, dd, *J* = 2.0, 5.0 Hz, 6-H), 8.86 (1H, s, 9-H) 8.92 (1H, s, 8-H) OH proton was not observed.

^{13}C-NMR (100.53 MHz; $(CD_3)_2SO$): δ 28.9 (C-12), 80.2 (C-11), 108.0 (C-3), 115.8 (C-5), 139.6 (C-4), 152.9 (C-6), 156.7 (C-10), 160.8 (C-2), 168.9 (C-7).

IR: ν_{max}/cm^{-1} 3301 (m, N-H stretch, secondary amine) 3117 (m, N-H stretch, primary amine) 2996 (m, O-H stretch, carboxylic acid), 1681 (s, C=O stretch, carboxylic acid).

2.3.3.6 Synthesis of succinimidyl 2-BOC-hydrazinopyridine-3-carboxylic acid; 'NHS-HYNIC-BOC'[21]

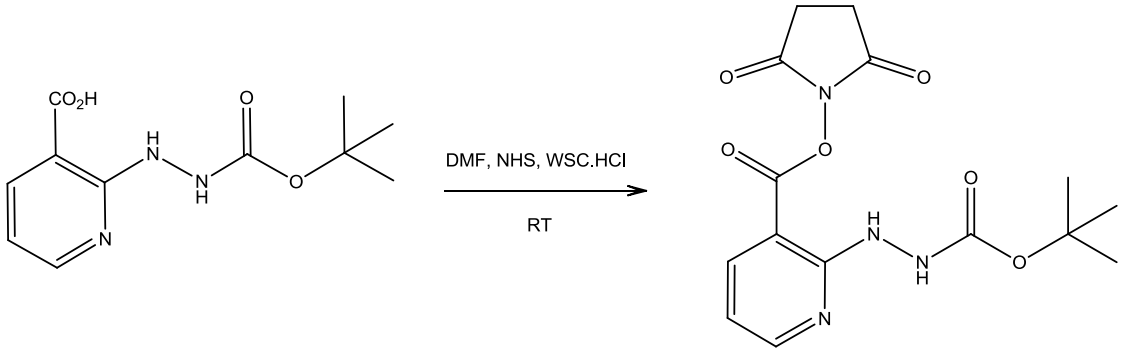

Scheme 2.8: Reaction sequence for the preparation of Succinimidyl 2-BOC-hydrazinopyridine-3-carboxylic acid.

To a solution of 2-BOC-hydrazinopyridine-3-carboxylic acid (0.1 g; 0.39 mmol) and N-hydroxysuccinimide (0.05 g; 0.39 mmol) in DMF (4 ml) was added a solution of WSC.HCl (water soluble carbodiimide hydrochloride) (0.08 g; 0.39 mmol) in DMF (2 ml). The reaction mixture became cloudy after 1 hour and stirring was continued for 16 hours at room temperature. The reaction mixture was filtered and the filtrate was concentrated to dryness to give a brown residue. The residue was dissolved in a minimum amount of ethyl acetate and passed through silica gel 60 (230-400mesh) using ethyl acetate as an eluant. The eluate was concentrated to dryness to give 0.09 g of a yellow solid, which was recrystallized from ethyl acetate/hexanes. ^{1}H NMR indicated that the reaction was unsuccessful and due to time constraints, it could not be attempted again in order to successfully synthesise 'NHS-2-HYNIC-BOC.

2.4 Results and Discussion

Both 2-hydrazinopyridine-3-carboxylic acid (2-HYNIC), 6-hydrazinopyridine-3-carboxylic acid (6-HYNIC) and their BOC-protected forms were synthesised successfully and obtained in high yields following modified methods of Abrams[1] and Slader.[20] The activated ester form of 6-BOC-HYNIC was also successfully synthesised however the activated ester form of 2-BOC-HYNIC was unsuccessful.

2.4.1 6-HYNIC

The commercially available and cheap 6-chloronicotinic acid was chosen as the starting material for the synthesis of 6-HYNIC. 6-hydrazinopyridine-3-carboxylic acid was formed *via* an aromatic substitution reaction using 80% hydrazine hydrate in 74% yield compared to 77% in the literature. Melting point, IR spectroscopy and ^{1}H and ^{13}C-NMR were used to analyse the identity and purity of the compound. The melting point of 285-288°C (literature 292-293°C) indicates the purity of the compound. The NMR and IR spectra elucidate the structure of the compound.

The synthesis of 6-HYNIC required several attempts and modifications to the literature preparation in order to be successful. The literature calls for 8.0g of 6-chloronicotinic acid to be added to 35ml of hydrazine hydrate and placed in a 100°C oil bath for 4 hours. It was decided that 6-HYNIC would be prepared initially according to the literature but on a smaller scale; 0.5417g of 6-chloronicotinic acid was added to 2.427ml of hydrazine hydrate. The literature indicated that after cooling to room temperature and concentrating to dryness, a white solid would be formed, however a yellow solid was obtained. The method also stated that the solid should be dissolved in water and acidified to pH 5.5 to give a precipitate, however none formed. At this stage it was unclear why a precipitate did not form at pH 5.5 so the acidification with HCl was continued until a yellow precipitate formed at pH 2.3. The precipitate was filtered and washed with 95% ethanol and ether and dried to give 1.4304g of product. ^{1}H-NMR did not confirm the product to be 6-HYNIC - the NMR spectrum shows one broad peak in the aromatic region. The only difference

between the starting material and the desired product is a substitution of the chloride for an amine group, therefore the signals observed in the NMR for the pyridine ring would also theoretically be present in the product. The solid was then recrystallised in water in an effort to remove any impurities to give 0.3203g of solid. Again the NMR was inconclusive.

At this stage it was unclear why the reaction was unsuccessful. Due to the small scale of the reaction, the yields were minimal and it could be that given this low yield, the precipitate was not obtained. It was decided that the reaction would be scaled up in order to obtain a significant quantity to isolate. The method was repeated as before, however this time 1.0201g of 6-chloronicotinic acid was added to 4.530ml of hydrazine hydrate and prepared according to previous method. During the acidification stage a viscous liquid formed rather than a precipitate. 0.2113g of solid precipitate was then isolated from the material. Again ^{1}H-NMR did not confirm the product to be 6-HYNIC (no corresponding peaks to literature data). Several further attempts and minor changes to the literature preparation were made to successfully synthesise 6-HYNIC.

In the successful preparation of 6-HYNIC, 1.0201g of 6-chloronicotinic acid and 4.530ml of hydrazine hydrate were added, under an inert atmosphere, and the reaction mixture was acidified to pH 3.0. 0.72g (74% yield) of a yellow solid formed and ^{1}H NMR spectrum confirms the product to be 6-HYNIC.

In the ^{1}H-NMR spectrum of 6-HYNIC **(see figure 2.3)**, six proton peaks are detectable, as is expected. The first peak in the aromatic region of the NMR spectrum is the aromatic proton 5-H, which is detected at 6.94 ppm, and is a doublet with a coupling constant of 8.4Hz. Further downfield, the 4-H proton in the pyridine ring, is determined by a peak at 8.07 ppm which is a double doublet with coupling constants of 2.0Hz and 8.4Hz. The coupling between the neighbouring protons 4-H and 5-H is shown by the same coupling constant. 4-H also couples with another proton shown by the coupling constant 2.0Hz. The 4-H proton has a higher chemical shift than the 5-H proton, this is due to it's proximity to the carboxylic acid group, which has an electron withdrawing effect. Further downfield, there is a doublet peak at 8.63 ppm which determines the aromatic proton 2-H. This 2-H proton has a

coupling constant of 2.0Hz and shows long range coupling between the 2-H proton and the 4-H proton. The 2-H proton is further downfield, i.e. has a higher chemical shift, than the 4-H proton due to it's proximity to the nitrogen in the ring, which also has an electron withdrawing effect. The 4-H and 5-H protons are shifted further downfield due to the resonance effect. Resonance structures will leave a lack of electron density in the *ortho* and *para* positions with respect to the carboxylic acid group. The carboxylic acid proton was observed in this spectrum as a broad singlet at 10.24 ppm, which is where it is expected (10-13 ppm). The 8-H and 9-H protons on the NH_2 group were observed as a very broad signal ranging from 2.5 ppm to 4.5 ppm. O-H and N-H protons are not always observed in NMR spectra as their presence is concentration dependant and their position can alter in the spectrum. Unlike carbon bonded protons, N-H and O-H protons do not tend to couple with their neighbouring protons.

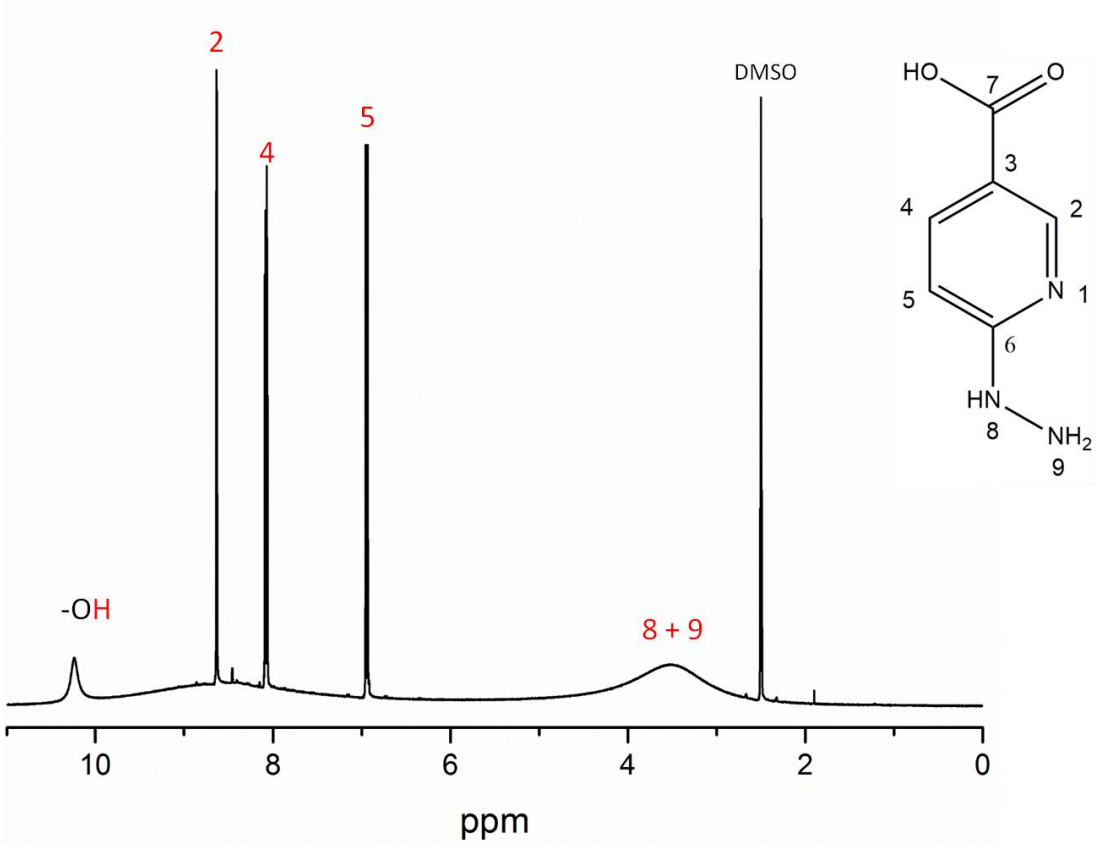

Figure 2.3: ^{1}H NMR spectrum of 6-HYNIC.

The ^{13}C-NMR spectra for 6-HYNIC shows six carbon peaks, as expected. Using the same numbering system as for the ^{1}H-NMR interpretation, C-5 is shown at 108.9 ppm, C-4 is shown at 138.9 ppm, and C-2 is shown at 148.0 ppm. Again, C-2 is furthest downfield, followed by C-4 and C-5. C-3 and C-6 are not bonded to a proton, and are shown at 118.6 ppm and 158.1 ppm respectively. The C-3 carbon is in *para* position to the hydrazine group which is electron donating and therefore has a lower chemical shift due to the added electron density. This added electron density shields the carbon from the magnetic field. The opposite is true for the carbon at C-6. The C-6 carbon at 158.1 ppm is in *para* position to the carboxylic acid group, which has an electron withdrawing effect. The lack of electron density means that C-6 is not shielded from the magnetic field and consequently has a higher chemical shift. The peak at 166.0 ppm determines the C-7 carbon of the carboxylic acid group. This carbon has a high chemical shift due to the electronegative oxygens on the carboxylic acid group.

The IR spectrum for 6-HYNIC shows each of the functional groups that are expected; 3350 (m, N-H stretch, secondary amine) 3223 (m, N-H stretch, primary amine), 2691 (m, O-H stretch, carboxylic acid), 1663 (s, C=O stretch, carboxylic acid). These functional groups are all present in the structure of HYNIC and help to identify the compound as 6-HYNIC. Not every peak present in the spectra is noted here, just enough peaks to indicate the correct functional groups in the spectra for all compounds.

The results of the ^{1}H and ^{13}C-NMR and IR spectroscopy confirm the successful synthesis of 6-HYNIC.

2.4.2 6-BOC-HYNIC

6-HYNIC was further reacted with di-tert-butyldicarbonate in triethylamine (TEA) to give 6-BOC-hydrazinopyridine-3- carboxylic acid in 98% yield. Melting point,

IR spectroscopy and ^{1}H and ^{13}C-NMR were used to analyse the identity and purity of the compound. The melting point of 142-145°C indicates the purity of the compound. The NMR and IR spectra confirm the structure of the compound.

The literature preparation calls for 2.13g of di-tert-buty dicarbonate to be added to a solution of 1.40g of 6-HYNIC and 1.2ml of triethylamine in 10ml DMF. Due to a limited supply of the starting material (the previously sunthesised 6-HYNIC), the reaction was scaled down and instead, 0.1425g of di-tert-buty dicarbonate was added to a solution of 0.10g of 6-HYNIC and 0.109ml of triethylamine in 1ml of DMF. This reaction mixture was stirred for 17 hours at room temperature. According to the literature the reaction mixture should then be concentrated to dryness under reduced pressure however the solid was not separated as it was not possible to successfully remove the solvent, even with gentle, and then more vigorous heating.

The synthesis was attempted again and, as before, 0.1425g of di-tert-buty dicarbonate was added to a solution of 0.10g of 6-HYNIC and 0.109ml of triethylamine in 1ml of DMF. This reaction mixture was stirred for 19 hours at room temperature. The reaction mixture was concentrated to dryness under reduced pressure to give a yellowish solid (unlike the literature which states that a brown solid is formed). According to the method, the solid should then be dissolved in ethyl acetate and passed through silica gel. Unfortunately, at this stage the solid obtained was found to be isoluble in ethyl acetate so a more polar solvent, methanol, was used. ^{1}H NMR indicated the presence of starting material and solvent rather than the desired product.

At this point it was uncertain as to why the reactions were unsuccessful; several further attempts and changes to the literature preparation were made to successfully synthesise 6-Boc-HYNIC. ^{1}H NMR spectra of subsequent syntheses either indicated the presence of starting material, suggesting the reaction did not go to completion, or were inconclusive.

In the successful preparation of 6-Boc-HYNIC, 1.07g (4.89 mmol) of di-tert-buty dicarbonate was added to a solution of 6-hydrazinopyridine-3-carboxylic acid (0.50 g; 3.26 mmol) and triethylamine (0.91 ml; 6.52 mmol) in DMF (8 ml) under an inert

atmosphere. The reaction mixture became homogeneous over 1 hour and stirring was continued for 16 hours at room temperature. The reaction mixture was concentrated to remove as much DMF as possible under reduced pressure to give a yellow solid. The resulting yellow paste was dissolved in a minimum amount of ethyl acetate and shaken in a separating funnel with 8 aliquots of saturated ammonium chloride solution (100 cm^3 each). The organic layer was dried with sodium sulfate and vacuum filtered to give a clear yellow solution. This was concentrated to dryness and dried in a vacuum oven (60°C, 24 hours) to yield a yellow solid which was used without further purification.

In the ^1H -NMR spectrum of 6-BOC-HYNIC, a singlet peak at 1.34 ppm determines the BOC group. This peak shows as a singlet due to the fact that all the protons in the CH_3 groups share the same environment and are therefore equivalent. This peak has a lower chemical shift than the other protons in the spectrum due to the electron donating effect of the three methyl groups on the BOC group. The aromatic protons; 5-H, 4-H and 2-H are detected at similar values to the ^1H -NMR spectrum of 6-HYNIC; 6.58 ppm, 7.92 ppm and 8.53 ppm respectively. The 8-H proton is observed as a singlet at 8.96 ppm, and the 9-H proton is observed as a singlet at 8.87 ppm. The 7-H proton is not observed in this spectrum. Neither the N-H protons nor the O-H protons are present in the literature NMR spectrum, but all other protons for 6-BOC-Hynic are in good agreement with the literature.

The ^{13}C-NMR spectra for 6-BOC-HYNIC shows nine carbon peaks, as expected. The BOC group carbon, C-12 is observed at 28.6 ppm, and the other BOC group carbon, C-11 is observed at 79.7 ppm. The C-11 carbon is shown at a higher chemical shift than the other BOC group carbons as it is next to an oxygen atom and has no hydrogens attached to it, therefore has less electron density. The C-10 carbon is observed at 156.4 ppm due to the proximity of the neighbouring oxygens which take the electron density away from the carbon, causing it to have a higher chemical shift. The other carbons are in the ^{13}C-NMR spectra are in good agreement with the previous carbons in the ^{13}C-NMR spectra for 6-HYNIC.

The IR spectrum for 6-BOC-HYNIC shows each of the functional groups that are expected; 3244 (m, N-H stretch, secondary amine) 2978 (m, C-H stretch), 1701, 1683 (s, C=O stretch, carboxylic acid), 1240, 1205, 1153 (s, C-O stretch, ester). These functional groups are all present in the structure of 6-BOC-HYNIC and help to identify the compound as 6-BOC-HYNIC.

2.4.3 NHS-HYNIC-BOC

6-BOC-HYNIC was further reacted with *N*-hydroxysuccinimide in the presence of WSC.HCl (water soluble carbodiimide hydrochloride) to give succinimidyl 6-BOC-hydrazinopyridine-3-carboxylic acid in 62% yield compared to 60% in the literature. Melting point, IR spectroscopy and ^{1}H and ^{13}C-NMR were used to analyse the identity and purity of the compound. The melting point of 166-167°C (literature 169.5-172°C) indicates the purity of the compound. The NMR and IR spectra elucidate the structure of the compound.

The protons in the ^{1}H-NMR spectrum of NHS-6-HYNIC-BOC are in good agreement with the protons from the 6-BOC-HYNIC spectrum. The succinimidyl CH_2 (14-H) protons are determined by a singlet peak at 2.83 ppm. The peak for the 14-H protons is shown as a singlet because the four succinimidyl protons are equivalent. The two N-H protons, 8-H and 9-H, have shifted to a slightly higher chemical shift when compared with the ^{1}H-NMR spectrum of 6-BOC-HYNIC. All other proton peaks are in good agreement with the previous ^{1}H -NMR spectrum.

The ^{13}C-NMR spectra for NHS-6-HYNIC-BOC shows eleven carbon peaks as expected. The C-14 peak for the two succinimidyl carbons is shown at 24.8 ppm. The two carbonyl carbons, C-13, are observed at 162.7 ppm. C-12 is observed at 28.6 ppm, C-11 is observed at 80.5 ppm, C-5 is observed at 105.0 ppm, C-3 is observed at 112.8 ppm, C-4 is observed at 139.4 ppm, C-2 is observed at 150.9 ppm,

C-6 is observed at 156.4 ppm, C-13 is observed at 162.7 ppm, C-10 is observed at 168.9 ppm and finally, C-7 is observed at 170.4 ppm.

The IR spectrum for NHS-6-HYNIC-BOC shows each of the functional groups that are expected; 3361 cm^{-1} (m, N-H stretch, secondary amine) 2927 cm^{-1} (m, C-H stretch), 1734 cm^{-1}, 1717 cm^{-1} (s, C=O stretch, ester), 1647 cm^{-1}, 1601 cm^{-1} (s, C=O stretch, amide), 1240 cm^{-1}, 1206 cm^{-1}, 1153 cm^{-1} (s, C-O stretch, ester) . These functional groups are all present in the structure of NHS-6-HYNIC-BOC and help to identify the compound as NHS-6-HYNIC-BOC.

2.4.4 2-HYNIC

For the synthesis of 2-HYNIC, the commercially available and cheap 2-chloronicotinic acid was chosen as the starting material. 2-hydrazinopyridine-3-carboxylic acid was formed *via* an aromatic substitution reaction using 80% hydrazine hydrate in 51% yield. Melting point, IR spectroscopy and ^{1}H and ^{13}C-NMR were used to analyse the identity and purity of the compound. The melting point of 194-196°C indicates the purity of the compound. The NMR and IR spectra elucidate the structure of the compound.

The synthesis of 2-HYNIC proved to be less complex than the synthesis of 6-HYNIC although still non-trivial. Several modifications were made to the literature preparation, again, as with the other HYNIC analogues and derivatives, the reaction was scaled down initially which proved to be problematic in gaining a useful amount of product. 0.50 g of 2-chloronicotinic acid was added to 2.27 ml of hydrazine hydrate. ^{1}H NMR showed that reactions on this scale proved to be unsuccessful or inconclusive. Scaling up the procedure gave more promising results and in the successful synthesis of 2-HYNIC 1.01g of 2-chloronicotinic acid was add to 4.60 ml of 80% hydrazine hydrate. The reaction was undertaken according to a modified

literature preparation and 0.50 g of 2-hydrazinopyridine-3-carboxylic acid was given as an orange solid. ^{1}H NMR of this solid confirmed the structure of 2-HYNIC.

In the ^{1}H -NMR spectrum of 2-HYNIC **(see figure 2.4)**, all of the six expected proton signals are detected. The first peak in the aromatic region of the NMR spectrum is the aromatic proton 5-H, which is detected at 6.30 ppm, and is a double doublet with coupling constants of 5.2 Hz and 7.6 Hz. Further downfield, the 4-H proton in the pyridine ring, is determined by a peak at 8.04 ppm which is a double doublet with coupling constants of 2.0 Hz and 7.6 Hz. The coupling between the neighbouring protons 4-H and 5-H is shown by the same coupling constant (7.6 Hz). 4-H also couples with another proton as shown by the coupling constant 2.0Hz. The 4-H proton has a higher chemical shift than the 5-H proton, this is due to it's proximity to the carboxylic acid group, which has an electron withdrawing effect. Further downfield, there is a double doublet peak at 8.18 ppm which determines the aromatic proton 6-H. This 6-H proton has coupling constants of 2.0 Hz and 5.2 Hz and shows coupling with the neighbouring 5-H proton (5.2 Hz) as well as long range coupling between the 6-H proton and the 4-H proton (2.0 Hz). The 6-H proton is further downfield, i.e. has a higher chemical shift, than the 4-H proton due to it's proximity to the nitrogen in the ring, which also has an electron withdrawing effect. The 4-H and 6-H protons are shifted further downfield due to the resonance effect. Resonance structures will leave a lack of electron density in the *ortho* and *para* positions with respect to the carboxylic acid group. The carboxylic acid proton, -OH, was observed in this spectrum as a broad singlet at 9.31 ppm, which is about where it is expected. The 8-H and 9-H protons on the NH_2 group were observed between 4 and 5 ppm. O-H and N-H protons are not always observed in NMR spectra as their presence is concentration dependant and their position can alter in the spectrum. Unlike carbon bonded protons, N-H and O-H protons do not tend to couple with their neighbouring protons.

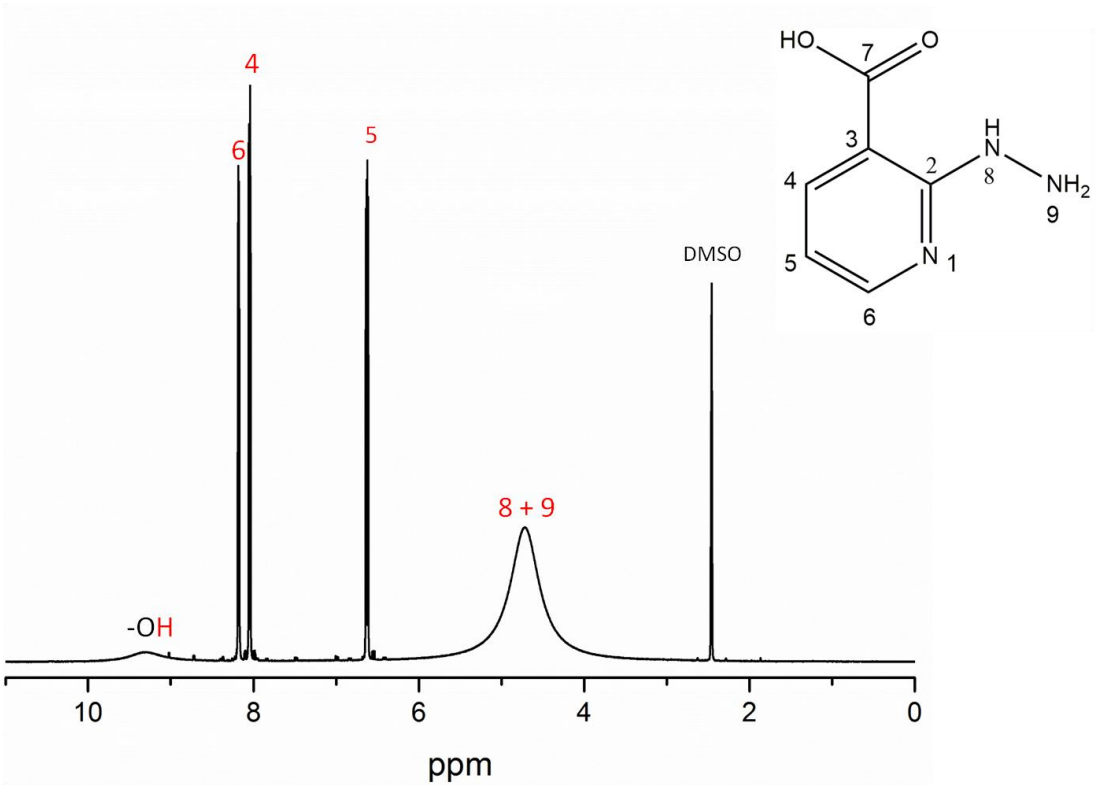

Figure 2.4: ^{1}H NMR spectrum of 2-HYNIC.

The ^{13}C-NMR spectra for 2-HYNIC shows six carbon peaks, as expected. C-5 is shown at 112.3 ppm, C-4 is shown at 140.9 ppm, and C-6 is shown at 150.8 ppm. C-6 is furthest downfield, followed by C-4 and C-5. C-3 and C-2 are not bonded to a proton, and are shown at 109.8 ppm and 159.4 ppm respectively. The C-3 carbon is in *ortho* position to the hydrazine group which is electron donating and therefore has a lower chemical shift due to the added elctron density. This added electron density shields the carbon from the magnetic field. The C-2 carbon is in *ortho* position to the carboxylic acid group, which has an electron withdrawing effect. The lack of electron density means that C-2 is not shielded from the magnetic field and consequently has a higher chemical shift. The peak at 168.7 ppm determines the C-7 carbon of the carboxylic acid group. This carbon has a high chemical shift due to the electronegative oxygens on the carboxylic acid group.

The IR spectrum for 2-HYNIC shows each of the functional groups that are expected; 3306cm^{-1} (m, N-H stretch, secondary amine) 3202 cm^{-1} (m, N-H stretch, primary amine), 2950 cm^{-1} (m, O-H stretch, carboxylic acid), 1655 cm^{-1} (s, C=O stretch, carboxylic acid). These functional groups are all present in the structure of HYNIC and help to identify the compound as 2-HYNIC. Not every peak present in the spectra is noted here, just enough peaks to confirm the correct functional groups in the spectra for all compounds.

The results of the ^{1}H and ^{13}C-NMR and IR spectroscopy confirm the successful synthesis of 2-HYNIC.

2.4.5 2-BOC-HYNIC

2-HYNIC was further reacted with di-tert-butyldicarbonate in triethylamine (TEA) to give 2-BOC-hydrazinopyridine-3- carboxylic acid in 86% yield. The reaction scheme for 2-HYNIC was adapted from the 6-HYNIC reaction scheme. Melting point, IR spectroscopy and ^{1}H and ^{13}C-NMR were used to analyse the identity and purity of the compound. The melting point of 165°C indicates the purity of the compound. The NMR and IR spectra elucidate the structure of the compound.

As with 6-Boc-HYNIC, several attempts were necessary to give the optimum reaction conditions for the synthesis of 2-Boc-HYNIC. Temperature, time, solvent choice, scale and molar ratios were all varied in an effort to obtain a successful product.

In the ^{1}H -NMR spectrum of 2-Boc-HYNIC, a singlet peak at 1.42 ppm determines the Boc group. This peak shows as a singlet due to the fact that all the protons in the CH_3 groups share the same environment and are therefore equivalent. This peak has a lower chemical shift than the other protons in the specrum due to the electron donating effect of the three methyl groups on the Boc group. The aromatic protons;

5-H, 4-H and 6-H are detected at similar values to the ^{1}H-NMR spectrum of 2-HYNIC. The 8-H proton is observed as a singlet at 8.86 ppm, and the 9-H proton is observed as a singlet at 8.92 ppm. The 7-H proton is not observed in this spectrum. Neither the N-H protons nor the O-H protons are present in the literature NMR spectrum, but all other protons for 2-Boc-Hynic are in good agreement with the literature.

The ^{13}C-NMR spectra for 2-Boc-HYNIC shows nine carbon peaks, as expected. The BOC group carbon, C-12 is observed at 28.9 ppm, and the other BOC group carbon, C-11 is observed at 80.2 ppm. The C-11 carbon is shown at a higher chemical shift than the other BOC group carbons as it is next to an oxygen atom and has no hydrogens attached to it, therefore has less electron density. The C-10 carbon is observed at 156.7 ppm due to the proximity of the neighbouring oxygens which take the electron density away from the carbon, causing it to have a higher chemical shift. The other carbons are in the ^{13}C-NMR spectra are in good agreement with the previous carbons in the ^{13}C-NMR spectra for 2-HYNIC.

The IR spectrum for 2-Boc-HYNIC shows each of the functional groups that are expected; 3301 (m, N-H stretch, secondary amine) 3117 (m, N-H stretch, primary amine) 2996 (m, O-H stretch, carboxylic acid), 1681 (s, C=O stretch, carboxylic acid). These functional groups are all present in the structure of 2-Boc-HYNIC and help to identify the compound as 2-Boc-HYNIC.

2.4.6 Further Modifications to Literature Prep

Several attempts were necessary to successfully add the Boc protection group to the HYNIC analogues. Research of the literature in this area indicated that the ratio of reagents; chloronicotinic acid (1 equivalent), triethylamine (TEA) (1.2 equivalent) Boc (1 equivalent), is not optimum. Changing the ratio of moles of the starting materials improved the synthesis and yield of the obtained product. TEA is used in

this reaction to remove any salt formed; in this case hydrogen chloride is formed. The NMR spectra of several failed attempts at the synthesis of Boc-HYNIC indicated that there was still a significant amount of hydrogen chloride present at the end of the reaction. Increasing the ratio of TEA to chloronicotinic acid improved the synthesis of both 2-Boc-HYNIC and 6-Boc-HYNIC. The molar ratio of chloronicotinic acid to TEA recommended in the literature was 1:1.2. The molar ratio was changed to 1:2. In the case of 6-Boc-HYNIC, the yield was improved from 78% to 98%. The molar ratio of chloronicotinic acid to di-tert-butyldicarbonate was recommended to be 1:1 as per the literature. However after several failed attempts at this synthesis, the molar ratio was changed to 1:1.5 with the Boc in excess. This allowed the synthesis to proceed and the overall yield was improved.

In the synthesis of succinimidyl 6-Boc-hydrazinopyridine-3-carboxylic acid and succinimidyl 2-Boc-hydrazinopyridine-3-carboxylic acid, WSC.HCl (water soluble carbodiimide hydrochloride) was used as a coupling agent instead of dicyclohexylcarbodiimide (DCC) to prepare the active esters. WSC.HCl is a versatile coupling agent which can be used under aqueous conditions, and therefore offers a distinct advantage over DCC as it can easily be removed after reaction by washing out or extraction.

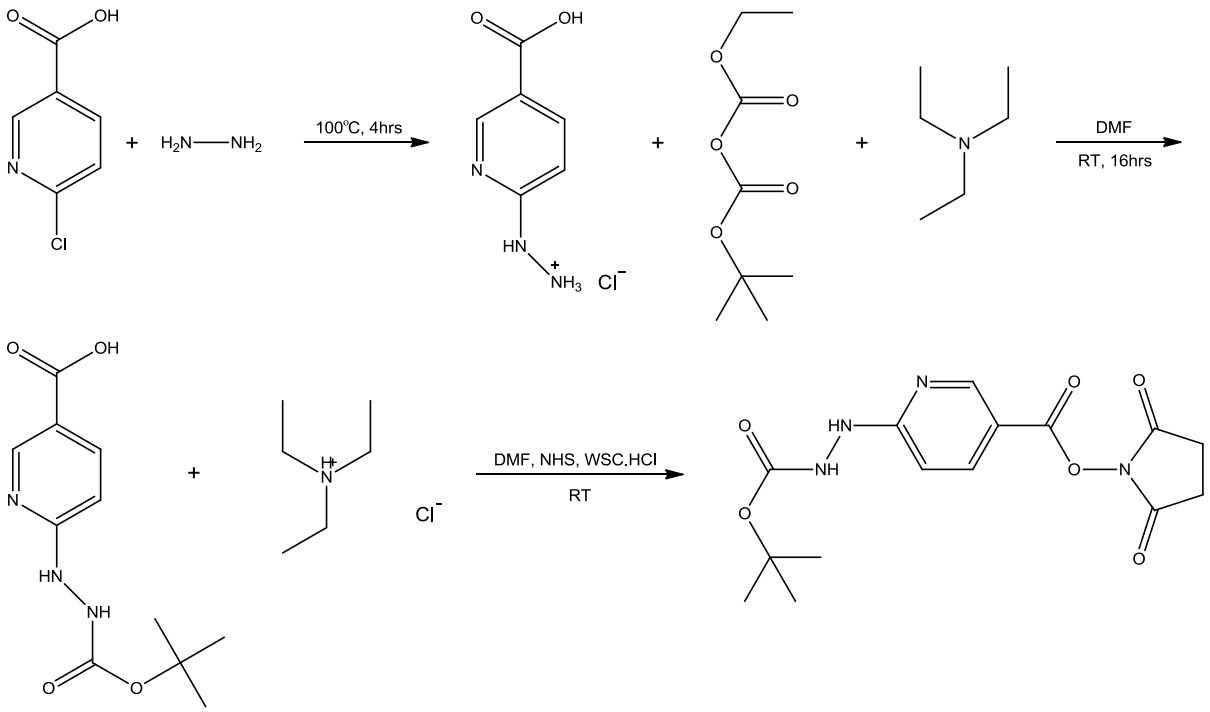

Scheme 2.9: Reaction scheme showing synthesis of Succinimidyl 6-Boc-hydrazinopyridine-3-carboxylic acid.

2.5 Conclusions and Future Work

The 6-hydrazinonicotinyl group, known as HYNIC, is an attractive bifunctional chelating agent for preparing ^{99m}Tc-labelled peptides and proteins for medical imaging. Two different HYNIC analogues (2-HYNIC and 6-HYNIC) and their BOC-protected forms were synthesised in high yields. The syntheses of these compounds are non-trivial and required multiple attempts and several changes to the literature methods. Preliminary experiments were performed, and ^{1}H-NMR and ^{13}C-NMR spectra for these reactions have shown to be either unsuccessful or inconclusive, demonstrating the limitations of the approach for synthesising HYNIC and its analogues.

6-HYNIC has been synthesised according to a modified prep in 74% yield. 6-Boc-HYNIC has been synthesised according to a modified prep in 98% yield. NHS-HYNIC-BOC has been synthesised according to a modified prep in 98% yield. 2-HYNIC has been synthesised according to a modified prep in 51% yield. 2-Boc-HYNIC has been synthesised according to a modified prep in 86% yield.

Due to time constraints of the project, the HYNIC analogues were not radiolabelled with technetium-99m, nor were the use of novel co-ligands to saturate the coordination sphere of technetium tested.

There are a number of variables to be explored in this field such as BFCs, radioisotopes, ligands and choice of targeting molecule. To start with, while 6-HYNIC has shown to be an important BFC in binding radiometals to target molecules, it is not without its limitations. One of the main areas of research concerns the uncertainty of the structure of the coordination sphere of the technetium core, specifically in how to optimise it to produce radiopharmaceuticals with the best convenience and efficiency of labelling, structural homogeneity, *in vivo* stability and targeting properties. 6-HYNIC cannot saturate the coordination sphere of technetium which means that the use of co-ligands is required. Co-ligands, such as tricine and EDDA, can modify the hydrophilicity and stability of the targeting

molecule.[14] Tricine, for example, allows for quick labelling and high specific activity under mild conditions, however, it produces a mixture of isomeric complexes.[6, 14] EDDA allows for improved stability and homogeneity but requires heating and does not easily coordinate directly with technetium-99m.[14, 22] Future work in this field could include the design of alternative co-ligands to satisfy the technetium-99m coordination sphere which allow for efficient labelling, high specific activity and stability, and reduced isomeric complexes, under mild conditions to allow for direct labelling with larger peptides and proteins.

Additionally, further HYNIC analogues such as 2-HYNIC and 4-HYNIC have yet to be fully explored. The use of 2-HYNIC as an efficient BFC for technetium-99m complexes may show promise. Meszaros et al. showed that the coordination chemistry of 2-HYNIC with technetium-99m is similar to the coordination chemistry of 6-HYNIC with technetium-99m.[21] While 6-HYNIC is widely used as a BFC for radiolabelling biomolecules including peptides and proteins, 2-HYNIC is not as widely used and has not yet been incorporated into peptides. Further research could include utilising the success of 6-HYNIC as a BFC for radiolabelling with technetium-99m, with a view to replicating that success with 2-HYNIC and determining whether 2-HYNIC gives analogous results to 6-HYNIC. 2-HYNIC may present a better profile for some radiopharmaceuticals.

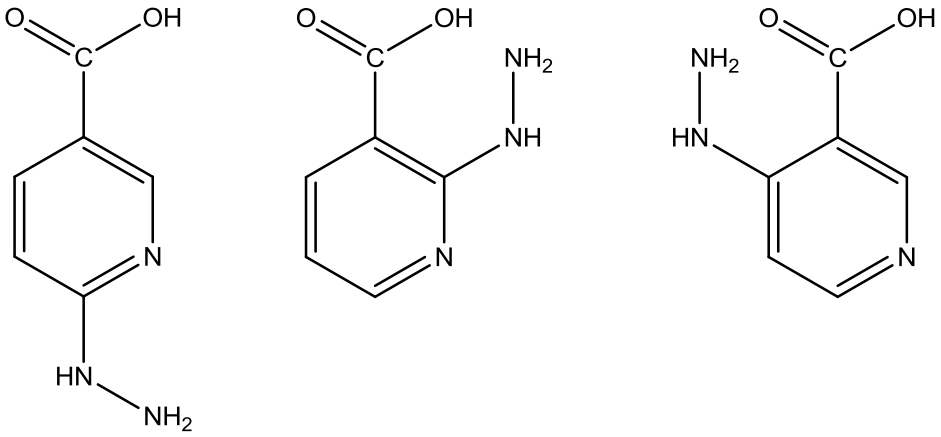

1 **2** **3**

Figure 2.5: HYNIC analogues; **(1)** 6-HYNIC, **(2)** 2-HYNIC, **(3)** 4-HYNIC

2.6 References

1. M. J. Abrams, M. Juweid, C. I. Tenkate, D. A. Schwartz, M. M. Hauser, F. E. Gaul, A. J. Fuccello, R. H. Rubin, H. W. Strauss and A. J. Fischman, *Journal of Nuclear Medicine*, 1990, **31**, 2022-2028.
2. M. Jamous, U. Haberkorn and W. Mier, *Molecules*, 2013, **18**, 3379-3409.
3. S. Rajabifar, M. Akhlaghi, A. R. Jalilian, F. Bolourinovin, B. Maashkar, M. Talebimehrdar and M. Ghafouri, *Nukleonika*, 2009, **54**, 279-284.
4. C. Decristoforo and S. J. Mather, *Nuclear Medicine and Biology*, 1999, **26**, 389-396.
5. K. Bruus-Jensen, T. Poethko, M. Schottelius, A. Hauser, M. Schwaiger and H.-J. Wester, *Nuclear Medicine and Biology*, 2006, **33**, 173-183.
6. S. Liu, *Advanced Drug Delivery Reviews*, 2008, **60**, 1347-1370.
7. Y. Zhou, S. Chakraborty and S. Liu, *Theranostics*, 2011, **1**, 58.
8. A. Purohit, S. Liu, D. Casebier and D. S. Edwards, *Bioconjugate Chemistry*, 2003, **14**, 720-727.
9. R. C. King, M. B.-U. Surfraz, S. C. G. Biagini, P. J. Blower and S. J. Mather, *Dalton transactions (Cambridge, England : 2003)*, 2007, 4998-5007.
10. M. B. U. Surfraz, R. King, S. J. Mather, S. C. G. Biagini and P. J. Blower, *Journal of Medicinal Chemistry*, 2007, **50**, 1418-1422.
11. Y.-S. Kim, Z. He, W.-Y. Hsieh and S. Liu, *Bioconjugate Chemistry*, 2006, **17**, 473-484.
12. S. Liu, D. S. Edwards, R. J. Looby, A. R. Harris, M. J. Poirier, J. A. Barrett, S. J. Heminway and T. R. Carroll, *Bioconjugate Chemistry*, 1996, **7**, 63-71.
13. F. Yurt Lambrecht, K. Durkan, A. Özgür, C. Gündüz, Ç. B. Avci and S. Y. Susluer, *Journal of drug targeting*, 2013, **21**, 383-388.
14. L. K. Meszaros, A. Dose, S. C. Biagini and P. J. Blower, *Inorganica Chimica Acta*, 2010, **363**, 1059-1069.
15. Radiopharmaceuticals: Production and Availability, *51st International Atomic Energy Agency General Conference*, Vienna, 2007.
16. V. Mäde, S. Els-Heindl and A. G. Beck-Sickinger, *Beilstein journal of organic chemistry*, 2014, **10**, 1197-1212.
17. J. M. Palomo, *RSC Advances*, 2014, **4**, 32658-32672.

18. R. Weissleder and U. Mahmood, *Radiology*, 2001, **219**, 316-333.
19. M. Fani, H. Maecke and S. Okarvi, *Theranostics*, 2012, **2**, 481.
20. H. Slader, New strategies for the introduction of 18F into peptides for imaging with Positron Emission Tomography, University of Kent, 2009.
21. L. K. Meszaros, A. Dose, S. C. G. Biagini and P. J. Blower, *Dalton Transactions*, 2011, **40**, 6260-6267.
22. S. Liu, W.-Y. Hsieh, Y.-S. Kim and S. I. Mohammed, *Bioconjugate Chemistry*, 2005, **16**, 1580-1588.

Chapter 3 - Synthesis of POEGMA-*co*-PAMA for Binding with HYNIC

3.1 Introduction to Polymers

A polymer is defined as a large molecule constructed of many smaller repeating structural units, called monomers, that are covalently bonded together.[1, 2] The term polymer derives from the Greek 'poly' meaning 'many' and 'mer' meaning 'units'. Monomers possess two or more bonding sites, through which they can be linked to other monomers to form the chain. The chemical bonds within the chain are very strong and directional along the chains; linear chains are most easily produced, however, chains can be linked together, by changing the chemistry involved, i.e. the use of polyfunctional monomers, to produce branched and network structures.[3]

Formally, polymers that contain only one species of monomer are called homopolymers **(see figure 3.2 - A)**.[4] Although polymers which contain a single type of repeat unit, containing one or more monomer species, are also termed homopolymers.[5] An example of a homopolymer, is poly(methyl methacrylate), (PMMA), which is named for its monomeric composition; PMMA is made up of repeating units of the methyl methacrylate monomer **(see figure 3.1)**. The number of repeating units, in the polymer chain is termed the degree of polymerisation, DP.[2] The higher the DP the higher the molecular weight.[6] Here, *n* represents the number of repeating units:

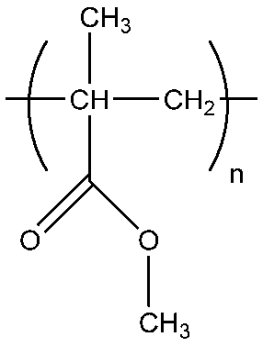

Figure 3.1: Methyl methacrylate subunit in a poly(methyl methacrylate) polymer.

Polymers can be separated into two classes: natural polymers and synthetic polymers. Examples of synthetic polymers include nylon and poly(vinyl chloride) (PVC). Examples of naturally occurring polymers include proteins, deoxyribonucleic acids (DNA) and cellulose.[7]

3.1.1 Copolymers

Chains that are composed of two different types of monomer are called copolymers. There are four main types of copolymers; statistical copolymers, alternating copolymers, block copolymers and graft copolymers.[8-10]

Alternating copolymers **(see figure 3.2 - C)** are characterised by the regular alternating placement of the two monomers (in equimolar composition) along the chain.[11] Special reaction conditions are necessary for producing alternating copolymers making this type of copolymer relatively rare. They are virtually impossible to produce by a free radical route and require pairs of monomers with highly specific copolymerisation reactivity ratios. The synthesis of alternating copolymers gives homogeneous systems that display properties representing a weighted average of the two repeat units.[12]

Block copolymers **(see figure 3.2 - B)** are comprised of substantial sequences or blocks of each monomer. The chemically distinct polymer chains are linked together at one or more intersections through covalent or non-covalent bonds. Block copolymers tend to show characteristic properties of the constituent homopolymers. They are usually prepared from living chain polymers or from step-growth systems which allow the control of block integrity and sequential architecture that is so important for achieving the desirable properties.[5, 12, 13]

Graft copolymers **(see figure 3.2 - E)** are polymers in which blocks of one monomer are grafted onto a backbone of the other as branches.[1, 8] They can be described as chemically linked homopolymer pairs, and as such are similar to block copolymers; like block copolymers, graft copolymers tend to show characteristic properties of the constituent homopolymers. Graft copolymers are prepared by free-radical, anionic or cationic addition polymerisation. These copolymers provide the basis for many

commercially important polymers such as impact polystyrene and **acrylonitrile butadiene styrene** (ABS).[5, 12, 14]

Statistical copolymers **(see figure 3.2 - D)** are copolymers in which the distribution of the two monomers is random but influenced by the individual monomer reactivities. The two monomers are simultaneously copolymerised resulting in modifications to the mechanical and physical properties of the polymer. Choosing monomers with reactivity ratios close to 1 produces statistical copolymers. Statistical copolymers follow a specific statistical law such as Markovian statistics.[11, 15]

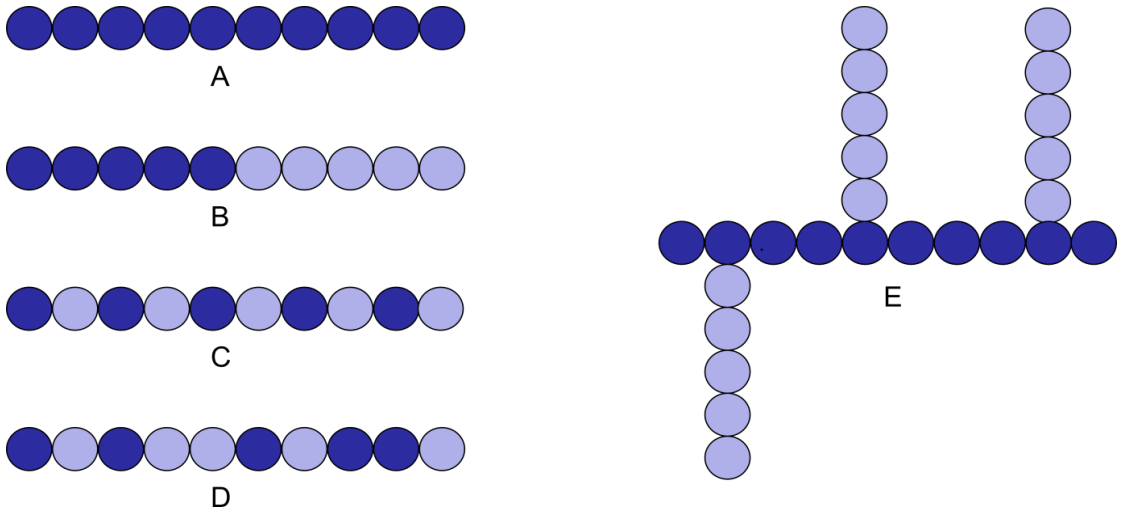

Figure 3.2: Representation of the different types of polymer; (A) a homopolymer, (B) block copolymer, (C) alternating copolymer, (D) statistical copolymer, (E) graft copolymer.

Copolymers are produced to give improved properties as they often exhibit a combination of the best properties of their components. An example is the copolymerisation of styrene with methyl methacrylate which improves heat resistance.[3]

3.1.1.1 Block Copolymers

Block copolymers **(see figure 3.2)** contain at least two types of monomer that have been polymerised in succession so that each monomer sequence forms a different block. The blocks are connected by a covalent bond that is formed during the subsequent addition of a monomer block.[16]

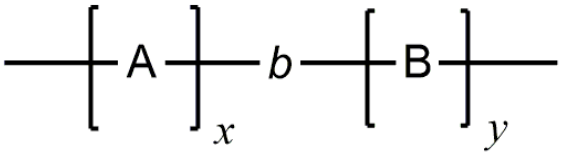

Figure 3.3: General notation for a block copolymer where A and B represent different monomer blocks, *b* is an abbreviation of block, and *x* and *y* represent the degree of polymerisation (DP).

Mixtures containing two or more homopolymers which are composed of chemically different monomers tend to undergo phase-separation.[17, 18] This is where the components separate resulting in poor overall properties of the mixture. It is therefore desirable to have a chemical bond between the two homopolymers to avoid separation. Block copolymers offer an advantage over other copolymers which is the ability to have polymers which are chemically different, and therefore incompatible, covalently bonded in the same macromolecule without undergoing macrophase separation. This means that the chemical and physical properties, such as hydrophobicity and thermal behaviour, of both blocks can be utilised.[17]

3.2 Polymerisation Techniques

Polymerisation is the process by which monomer molecules are converted into a polymer. The two most important types are step-growth polymerisation and chain-growth polymerisation.

3.2.1 Step-growth Polymerisation

Step-growth polymerisation usually, although not always, involves typical condensation reactions where a small molecule, e.g. H_2O or HCl is expelled as the link is built.

In step-growth polymerisation, a linear chain of monomer residues is obtained by the stepwise intermolecular condensation or addition of the reactive groups in bifunctional monomers. Any two molecular species in the mixture can react and the monomer is almost all incorporated into a chain molecule in the early stages of the reaction. In step-growth polymerisation, initiation, propagation and termination reactions are essentially identical in rate and mechanism. The chain length increases steadily as the reaction proceeds and long reaction times and high conversions are necessary for the production of a polymer with a large number-average chain length. The reaction rates for this type of polymerisation are slow at ambient temperatures but increase with a rise in temperature, although this has little effect on the chain length of the final product.[2, 5, 19]

3.2.2 Chain-growth Polymerisation

Chain-growth polymerisations involve the addition of unsaturated monomers where the special reactivity of π-bonds in the carbon to carbon double bond makes them susceptible to rearrangement if activated by free-radical or ionic initiators. The polymerisation proceeds in 3 steps: (1) *initiation*, when the active centre is created;

(2) *propagation*, involving growth of the chain by a kinetic chain mechanism; and (3) *termination*, where the kinetic chain is terminated by the neutralisation of the active centre. In chain-growth polymerisations, high degrees of polymerisation are attained at low monomer conversions and the average chain length shows little variation throughout the course of the polymerisation. The monomer concentration decreases steadily throughout the reaction. In this type of polymerisation, only the active centre can react with the monomer and add units onto the chain one after the other. Long reaction times increase the polymer yield, but not the molar mass of the polymer and an increase in temperature increases the rate of the reaction but decreases the molar mass.[2, 5, 19]

3.2.3 Free Radical Polymerisation

A free radical is a species containing an unpaired electron. The radical is capable of reacting with an olefinic monomer to generate a chain carrier that can propagate a macromolecular chain under the appropriate conditions.[20]

Free radical polymerisations proceed in four steps: (1) *initiation*, when the active centre is created; (2) *propagation*, where monomer molecules are added one by one to the active chain end. The reactive site is regenerated after each addition of monomer; (3) *transfer*, this occurs when an active site is transferred to an independent molecule such as a monomer, initiator, polymer, or solvent. This process results in both a terminated molecule and a new active site that is capable of undergoing propagation; (4) *termination*, where the eradication of active sites leads to "terminated" or inert, macromolecules. Termination occurs via coupling reactions of two active centres (combination), or atomic transfer between active chains (disproportionation).[20, 21]

Free radical polymerisation techniques can be conducted at a wide range of temperatures and in the presence of water and as such they provide a viable synthetic method for the production of large molecular weight polymers on an industrial scale. However, free radical polymerisation techniques offer no control over the degree of

polymerisation, molecular weight distribution and topology of the resulting polymers. Chain transfer may occur for every radical at any and all degrees of polymerisation and the influence of chain transfer on the average degree of polymerisation and on polydispersity carries enormous consequences. The initiation step can be slow compared with propagation due to the inefficient radical formation for some initiators. High concentrations of radical species in solution are undesirable because this increases the probability of bimolecular termination. This frequent termination means that there are no polymer chain ends able to continue with the propagation process. Consequently, traditional free radical polymerisation techniques cannot be used to produce more complex polymers such as block copolymers.[22, 23]

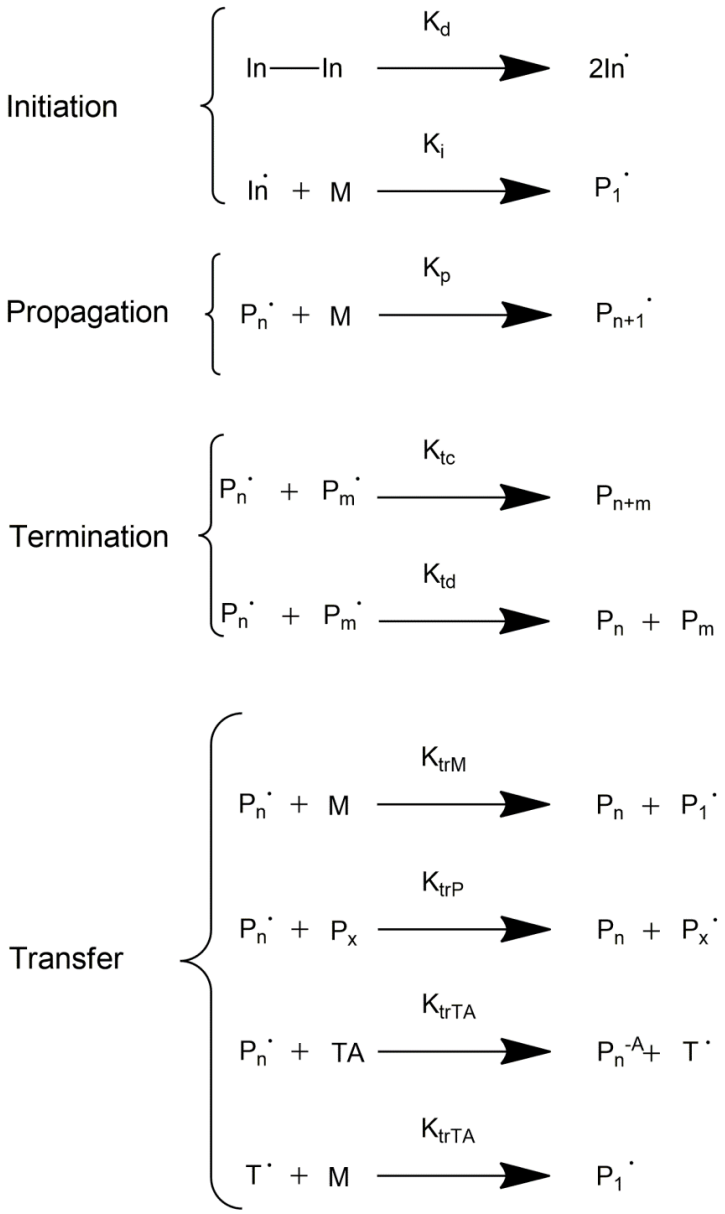

Figure 3.4: Reaction steps of a free radical polymerisation. Where, In = initiator, M = monomer, P = polymer, TA = transfer agent, K_d = rate of dissociation, K_i = rate of initiation, K_p = rate of polymerisation, K_{tc} = rate of termination via coupling, K_{td} = rate of termination via disproportionation, K_{trM} = rate of transfer to monomer, K_{trP} = rate of transfer to polymer and K_{trTA} = rate of transfer to transfer agent.

3.2.4 Controlled and Living Polymerisation Techniques

In order to maintain a low concentration of free radicals in solution, (enabling the formation of polymers with more complex compositions) techniques allowing for the reversible deactivation of free radicals have been developed. Living/controlled polymerisations may include slow initiation, reversible formation of species with various activities and lifetimes, reversible formation of inactive species, and/or reversible transfer.

Controlled living free radical polymerisations can be divided into several main types; stable free radical polymerisation (SFRP); atom transfer radical polymerisation (ATRP); nitroxide-mediated polymerisation (NMP) and reversible addition-fragmentation chain transfer polymerisation (RAFT).[24]

Living polymerisations must not include irreversible deactivation and irreversible transfer. These controlled free radical polymerisations (CRPs) yield polymers with well-defined composition and molecular weights, narrow polydispersities and controlled topology and functionality. The criteria for polymerisation to be termed as 'living' (as defined by Quirk and Lee)[25] are as follows:

1. The growth of the chain continues until all the monomer has been used up.
2. The molecular weight increases proportionally with conversion.
3. The concentration of the active species is constant regardless of the level of conversion.
4. The polydispersities are low.
5. The block copolymers are synthesised by sequential monomer addition.
6. The polymer chain ends maintain functionality.

3.2.4.1 Reversible Addition-Fragmentation chain Transfer (RAFT)

Reversible Addition-Fragmentation chain Transfer or RAFT polymerisation is one of several living or controlled radical polymerisation techniques. Other examples being atom transfer radical polymerisation (ATRP) and nitroxide-mediated polymerisation

(NMP). RAFT polymerisation was first developed at CSIRO in 1998.[24] It soon became the focus of intensive research, since the method allows synthetic tailoring of macromolecules with complex architectures with predetermined molecular weights. RAFT is among the most successful CRP techniques due to its applicability to a wide range of monomers. Exchange reactions in this particular technique are very fast which lead to well controlled systems.[26] The RAFT process involves conventional free radical polymerisation in the presence of a suitable chain transfer agent (RAFT agent). Some examples of commonly used RAFT agents include thiocarbonylthio compounds such as dithioesters, thiocarbamates, and xanthates, which are used to mediate the polymerisation via a reversible chain-transfer process. RAFT polymerisation can be applied to a wide range of monomers under a large number of experimental conditions, including the preparation of water-soluble materials. As with other controlled radical polymerisation techniques, RAFT polymerisations can be performed with conditions to favour low polydispersity indices and a predetermined molecular weight.[27] RAFT polymerisation can be used to design polymers of complex architectures, such as linear block copolymers, comb-like, star, brush polymers and dendrimers.[28]

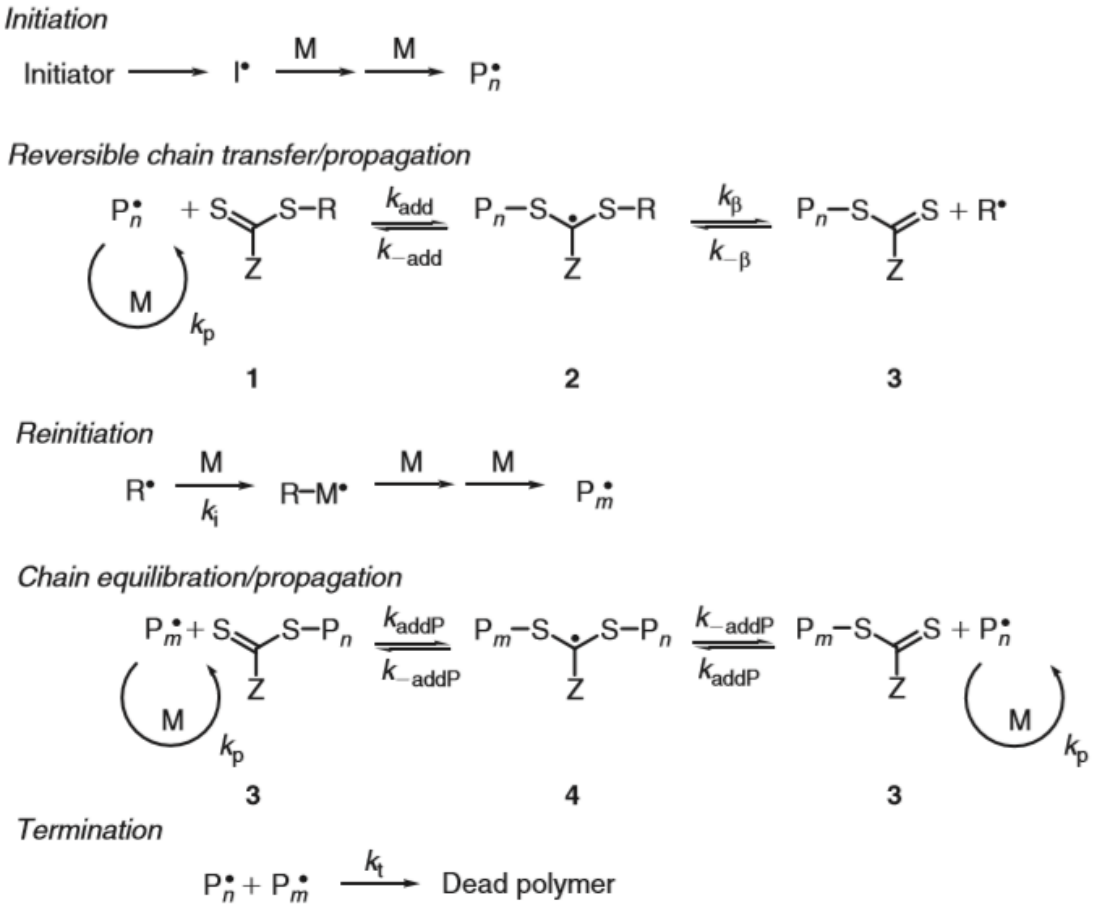

Scheme 3.1: Mechanism for RAFT polymerisation.[29]

3.2.5 Reaction Components

3.2.5.1 The RAFT Agent

The choice of RAFT agent should pay particular attention to the monomer being polymerised and the reaction conditions for the polymerisation. RAFT agents typically contain a thiocarbonylthio group (S=C-S) with substituents R and Z that

impact the reaction kinetics and the degree of structural control in the polymerisation.[30] Initiation is achieved using conventional thermal, photochemical or redox methods and the correct choice of RAFT agent for the monomer and the reaction conditions will determine the success of the polymerisation reaction.

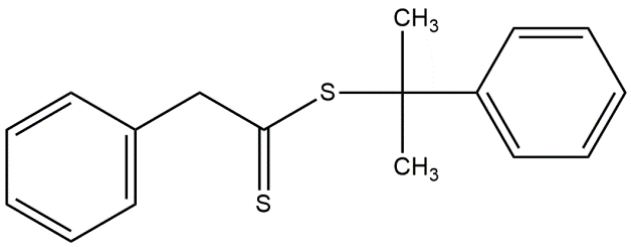

Figure 3.5: Raft agent 2-phenylprop-2-ylphenyldithioacetate (PPPDTA).

3.2.5.2 Monomers

One of the main advantages of using RAFT polymerisation over other controlled living free radical polymerisation techniques is the compatibility with a wide range of monomers. RAFT polymerisation is compatible with a much wider range of monomers than ATRP, from common monomers such as styrene to functioned monomers such as acrylic acid and even electron donating monomers such as vinyl esters.

3.2.5.3 Reaction Temperatures

There is an optimum temperature range for each monomer polymerised under RAFT conditions which depends on the nature of the monomer as well as the RAFT agent used. The rate of polymerisation increases with the greater temperature due to the

increase in the radical propagation rate constant. The activation energy of propagation is higher than the activation energy of radical termination; therefore the k_p/k_t ratio will increase, consequently improving the control over the system. However, at higher temperatures, chain transfer and other side reactions become more likely, so the optimum temperature range will take this into account.

3.2.5.4 Reaction Time

The reaction time for a particular polymerisation will have an effect on the molecular weight distributions and the polymer architecture. The rate of propagation will slow down as the polymerisation reaches completion; however, any side reactions occurring will be independent of the monomer concentration and as such will continue at the same rate. Therefore, continued heating once all the monomer has been used is not recommended as it may affect the RAFT functionality, affecting block formation.

3.2.5.5 Solvents and Media

RAFT polymerisations can be carried out in a variety of media, such as in alcohols or aqueous solution, although polymerisations can also be carried out in bulk. The main factor to consider is the solubility of the monomer, RAFT agent and initiator in the chosen solvent. RAFT polymerisations are unaffected by the polarity of the solvent; successful polymerisations have been carried out in water, short-chain alcohols and non-polar solvents. The chosen solvent should have a low chain transfer constant.

3.3 Poly(Oligo(ethylene glycol)methacrylate) POEGMA

Poly(ethylene glycol) (PEG) is an uncharged, water-soluble, nontoxic, non-immunogenic polymer and is therefore the most applied synthetic polymer in the field of biomedical science.[31] Monomers composed of a (meth)acrylate moiety connected to a short poly(ethylene)glycol (PEG) chain are versatile building-blocks for the preparation of 'smart' macromolecules. Many of these monomers are commercial and can be easily polymerized by either anionic, free-radical, or controlled radical polymerisation. The CRP approach allows synthesis of well-defined PEG-based macromolecular architectures such as amphiphilic block copolymers and dense polymer brushes. Furthermore, the resulting polymers exhibit fascinating solution properties in aqueous medium. Depending on the molecular structure of their monomer units, non-linear PEG analogues can be either insoluble in water, readily soluble up to 100°C, or thermo-responsive. Thus, these polymers can be used for building a wide variety of modern materials such as biosensors, artificial tissues, smart gels for chromatography, and drug carriers.[32]

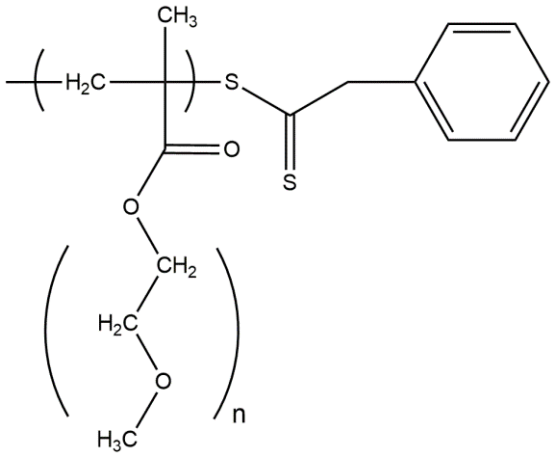

Figure 3.6: Structure of POEGMA**.**

3.4 Aims and Objectives

There is a recognized need to create well-defined polymer probes for *in vivo* and clinical PET and SPECT imaging to guide the development of new generation polymer therapeutics. "Polymer therapeutics", which can be used to describe polymeric drugs, polymer drug conjugates, polymeric micelles, polymer protein conjugates, and polyplexes, has become an emerging field of interest in both chemical and medical sciences over the last four decades. By introducing small radioactive probes into the polymeric system and using nuclear medicine imaging techniques such as positron emission tomography (PET) and single photon emission computed tomography (SPECT), pharmacokinetics, and distribution of the polymer therapeutic can be easily monitored.[33]

The aim is to synthesise a bifunctional copolymer (POEGMA-*co*-PAMA) which is biocompatible and can be attached to a HYNIC group and subsequently a peptide. The first step is to bind HYNIC to the copolymer, if that proves to be successful; a target specific receptor such as a short-sequence peptide will be attached. The aim is then to radiolabel the bifunctional copolymer with technetium-99 for SPECT.

With regards to the therapeutic effects of a polymer-based drug carrier system, the choice of backbone plays a crucial role. Essential requirements include biodegradability or biocompatibility with final excretion properties. The polymer must be well-defined in order to be developed as a polymer therapeutic. Fortunately, the introduction of living radical polymerisation techniques, such as ATRP and RAFT techniques have allowed well-defined polymer structures to become available. The RAFT technique offers access to different polymer architectures and various functional groups, for example, imaging moieties or therapeutics can be attached. This route allows for preparation of block copolymers of specific composition.[33]

Poly(oligo(ethylene glycol)methacrylate) (POEGMA) is chosen as the copolymer back bone as it is a biocompatible polymer.[32] Oligo(ethylene glycol)methacrylates (OEGMAs) are easily polymerisable using controlled radical polymerisation techniques such as atom transfer radical polymerisation (ATRP) and reversible addition-fragmentation chain transfer polymerisation (RAFT). The controlled

radical polymerisation of the OEGMA allows for a broad range of linear (homo, random, block), hyperbranched, dendric, and star (co)polymers.[28] The biocompatibility of the oligo(ethylene glycol) (OEG) pendant groups allows POEGMA based materials to be used in the biomedical fields.[32]

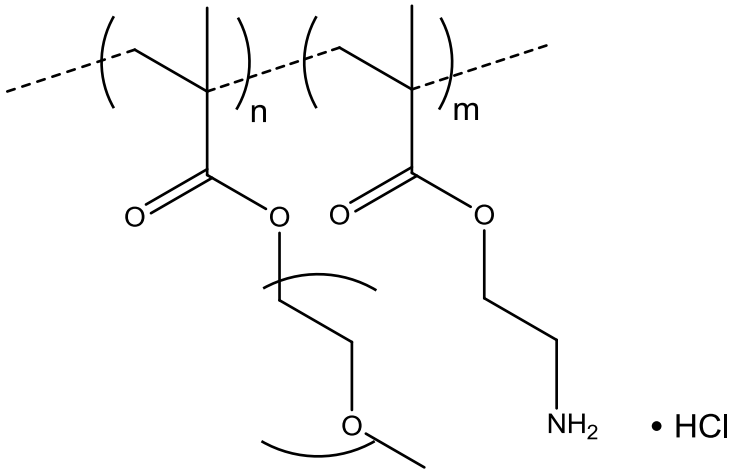

Figure 3.7: Structure of POEGMA-*co*-PAMA.

2-aminoethyl methacrylate hydrochloride can be added into the polymer structure as a comonomer. This will later allow for the binding of a copolymer to the HYNIC derivatives.

A suitable coupling strategy is essential since direct labelling of a molecule occurs only exceptionally. A linker must be labelled with the radionuclide of interest under conditions compatible with the stability of the labelled molecule; the label should be sufficiently stable under *in vivo* conditions; labelling should not affect the eventual specific binding ability of the biomolecule and non-specific interactions of the radioconjugate in organism should be as low as possible. The coupling strategy design depends on the character of the radionuclide binding - whether it is covalent binding (e.g. iodine radioisotopes) or chelation (metal ion radioisotopes)[34]

Once the copolymer POEGMA-*co*-PAMA has been synthesised it will need to be attached to the activated ester form of HYNIC. Active esters are improved

conjugation reagents which are prepared by the action of a dehydrating agent on a ligand containing a free carboxylic acid and a hydroxyl on a potential leaving group. The active ester reacts cleanly with deprotonated primary amines to form a very stable amide bond. The reaction can be carried out in aqueous conditions or using organic solvents. In this case, the conjugation will be achieved using EDC (1-ethyl-3-(3-dimethylaminopropyl) carbodiimide hydrochloride) coupling.

The short-sequence peptide will then be attached. The aim is to then radiolabel the bifunctional copolymer with technetium-99m for SPECT.

The advantage of attaching the radionuclide to a copolymer is that the number of binding sites is increased, making it a viable choice for radiolabelling applications. The chances of successfully imaging the point of interest, for example, a cancerous tumour where receptors are over-expressed, is therefore increased.

3.5 Experimental Section

3.5.1 Materials

Azobisisobutyronitrile (AIBN) was purchased from Molekula and used as received. Propanol (laboratory reagent grade) and chloroform (laboratory reagent grade) were purchased from Fisher and used without further purification. Aluminium oxide (activated, neutral, Brockmann 1, for chromatography, 50-200 μm) was purchased from Acros Organics. Polyoligo(ethylene glycol) methyl ether methacrylate (OEGMA) was purchased from Sigma Aldrich; to remove inhibitor OEGMA was run down an alumina oxide column. RAFT agent PPPDTA was synthesised according to literature method.[35] 2-aminoethyl methacrylate hydrochloride (AMA) (90%) was purchased from Aldrich and was purified by recrystallisation - AMA was dissolved in chloroform, filtered to remove insoluble impurities and dried under vacuum.

3.5.2 Instrumentation and Analysis

^{1}H and ^{13}C NMR: ^{1}H and ^{13}C nuclear magnetic resonance (NMR) spectra were recorded using a JEOL ECS-400 spectrometer at 30°C from solutions in $CDCl_3$.

GPC: Molecular weight characteristics of polymers were estimated relative to PMMA standards by gel permeation chromatography (GPC) using a PL-GPC 50 supplied by Polymer Laboratories Ltd, in conjunction with a refractive index detector. All determinations were carried out at 40°C with tetrahydrofuran (THF) as a mobile phase at a flow rate of 1 ml min-1, using a 50 mm x 7.8 mm 10 μm PLgel guard column and 2 x 300 mm x 7.8 mm 5 μm PLgel Mixed-C columns.

3.5.3 Polymeric Syntheses

3.5.3.1 A typical procedure for the RAFT synthesis of POEGMA with a degree of polymerisation (DP) of 50 units is given as follows;

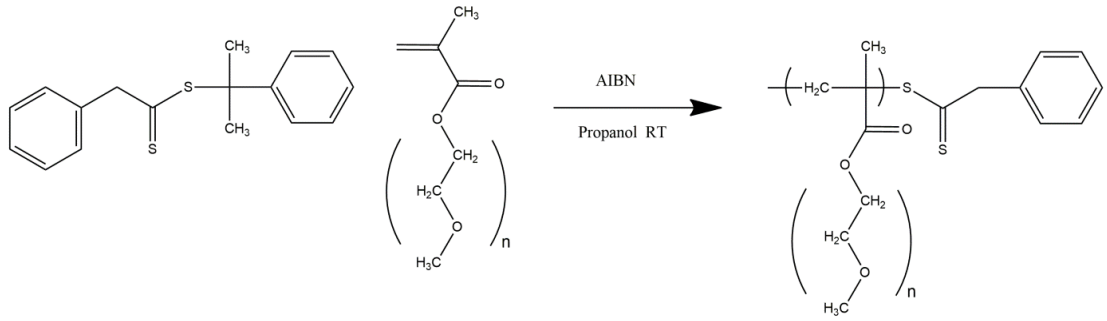

Scheme 3.2: Reaction sequence for the preparation of POEGMA.

Poly(ethylene glycol) methyl ether methacrylate (5.0g; 16.7mmol), RAFT agent 2-phenylprop-2-yl phenyldithioacteate (PPPDTA) (0.0895g; 3.34mmol), AIBN (0.6mg; 0.00366mmol) and propanol (5ml) were added to a Schlenk tube. The mixture was degassed through several freeze thaw cycles, sealed under vacuum and heated in a constant temperature bath at 70°C for 24 hours. The reaction mixture was exposed to air to stop the reaction. The product was retrieved by precipitation of the reaction mixture into hexane, filtered and dried under vacuum overnight to yield 4.2776g of POEGMA.

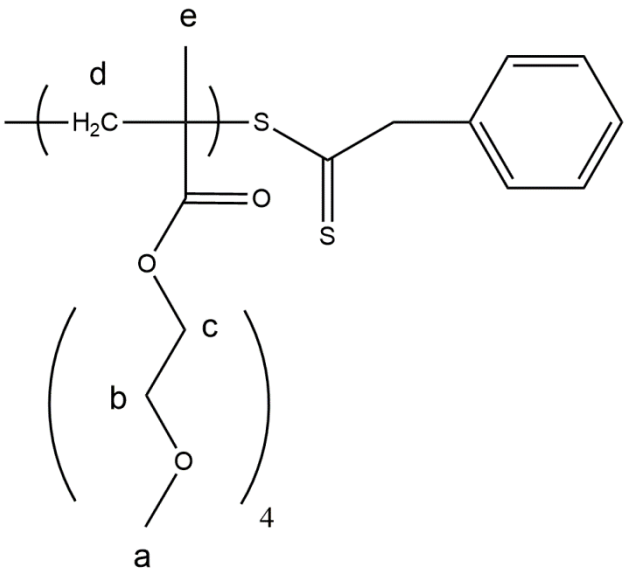

^{1}H-NMR (399.78 MHz; $(CD_3)_2SO$): δ 0.87 (s, e-H) 1.03 (s, e-H), 1.25 (s, e-H), 1.86 (q, d-H), 3.38 (s, a-H), 3.56 (s, b-H), 3.66 (s, b-H), 3.74 (t, b-H,) 3.56 (s, c-H).

3.5.3.2 A typical procedure for the RAFT synthesis of POEGMA-co-PAMA with 5% AMA is given as follows;

Poly(ethylene glycol) methyl ether methacrylate (5.00 g; 16.7 mmol), 2-aminoethyl methacrylate hydrochloride (0.138 g), RAFT agent PPPDTA (0.0895 g; 3.34 mmol), AIBN (0.6 mg; 0.00366 mmol), deionised water (1 ml) and propanol (4 ml) were added to a Schlenk tube. The mixture was degassed through several freeze thaw cycles, sealed under vacuum and heated in a constant temperature bath at 70°C for a predetermined time (**see table 3.1**). The reaction mixture was exposed to air to stop the reaction. The polymer product was retrieved by precipitation of the reaction mixture into hexane, filtered and dried under vacuum overnight.

3.5.3.2 A typical procedure for the RAFT synthesis of POEGMA-co-PAMA with 10% AMA is given as follows;

Poly(ethylene glycol) methyl ether methacrylate (5.00 g; 16.7 mmol), 2-aminoethyl methacrylate hydrochloride (0.275 g), RAFT agent PPPDTA (0.0895 g; 3.34 mmol), AIBN (0.6 mg; 0.00366 mmol), deionised water (1 ml) and propanol (4 ml) were added to a Schlenk tube. The mixture was degassed through several freeze thaw cycles, sealed under vacuum and heated in a constant temperature bath at 70°C for a predetermined time (**see table 3.1**). The reaction mixture was exposed to air to stop the reaction. The polymer product was retrieved by precipitation of the reaction mixture into hexane, filtered and dried under vacuum overnight.

The specific mechanism for the RAFT polymerisation of OEGMA is shown in **figures 3.3a** and **3.3b**. The homolytic fission of AIBN is shown resulting in two radical initiating species. The radical is then transferred from the initiator to an OEGMA monomer unit. This OEGMA monomer radical then combines with the RAFT agent allowing for the fragmentation steps to occur. Polymerisation can continue through the equilibrium of the active and dormant species until bimolecular termination occurs when two polymer chains meet.

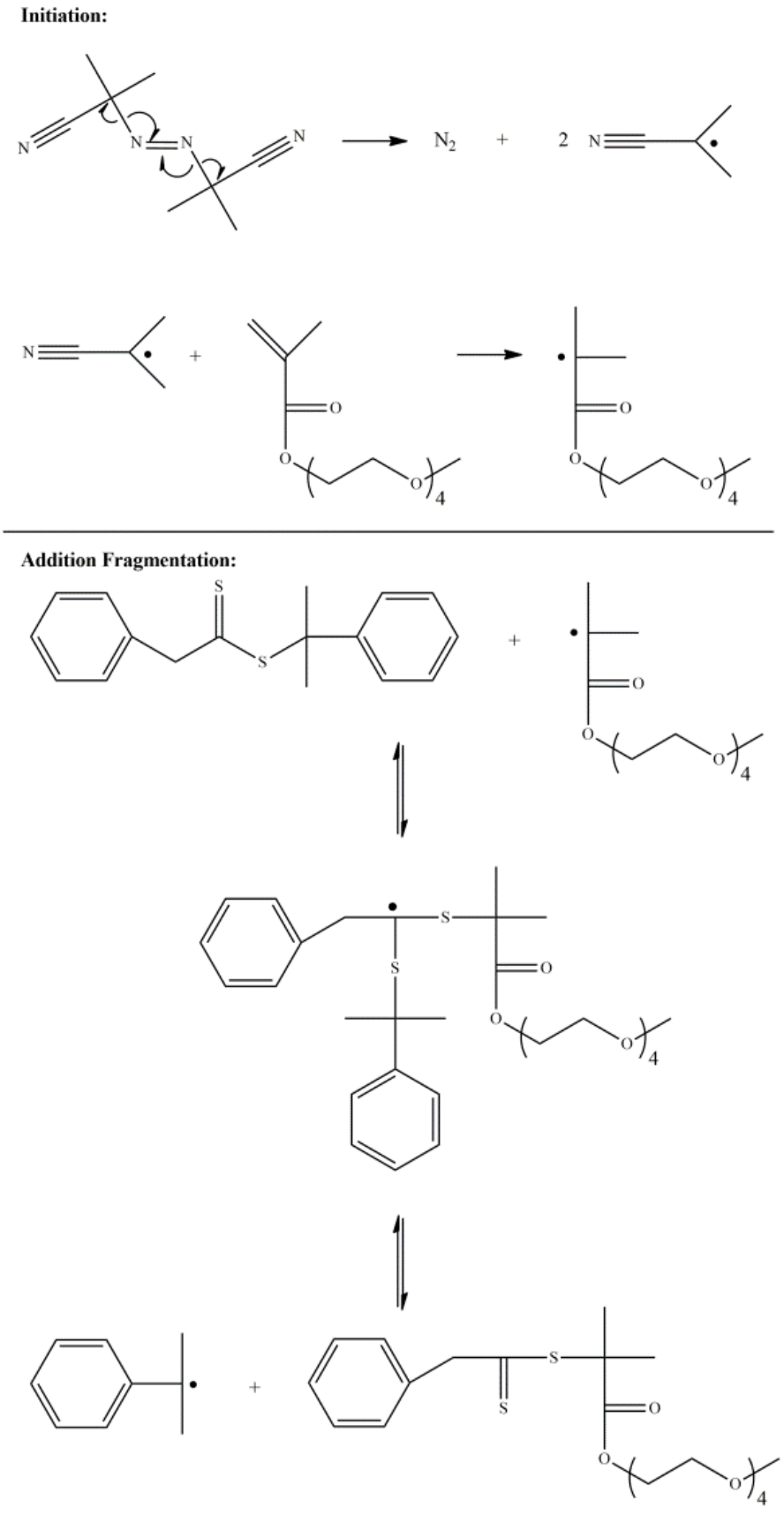

Scheme 3.3a: Mechanism for the synthesis of POEGMA by RAFT.

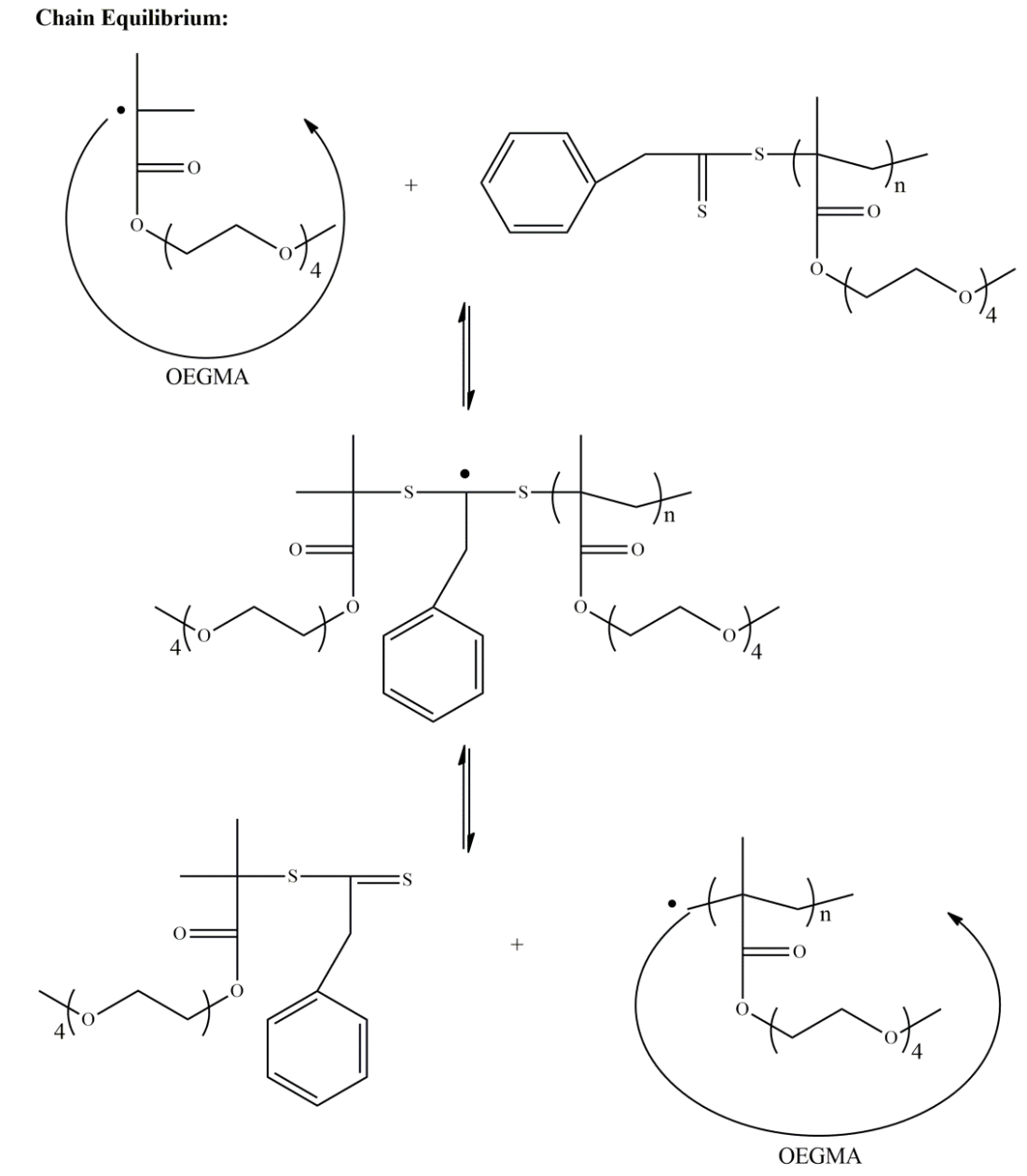

Scheme 3.3b: Mechanism for the synthesis of POEGMA by RAFT.

3.6 Results and Discussion

The reason for choosing RAFT as the method of polymerisation for the polymers presented in this work is due to its ability to synthesise polymers of controlled molecular weights and low polydispersity. There is an optimum chain length for every polymeric application which provides the best results for that particular application. In this case, *in vivo* studies would indicate which chain length would give the ideal transportation and binding. RAFT is therefore an ideal polymerisation technique for the synthesis of predetermined chain-length polymers.

RAFT agents are not currently commercially available and therefore need to be synthesised. The choice of RAFT agent depends on the monomer being polymerised and the reaction conditions for the polymerisation. 2-phenylprop-2-ylphenyldithioacetate (PPPDTA) **(see figure 3.2)** was selected as the RAFT agent in this work. This is due to the inclusion of a benzyl Z group which means the radical in the RAFT intermediate is in a less stable disulphur alkyl position when compared to the direct combination with the aromatic ring. This leads to a faster rate of fragmentation and results in a faster establishment of the RAFT equilibrium. This will allow the RAFT agent to mediate the polymerisations at ambient temperatures.

The RAFT agent was synthesised by a previous PhD student according to the method of Quinn and co-workers.[36]

The controlled radical polymerisation of OEGMA was performed in aqueous environment at 70°C and lead to the formation of the homopolymer POEGMA with a narrow molecular weight distribution ($M_w/M_n < 1.5$) **(see entry PO1, Table 3.1)**.

Table 3.1: Polymers synthesised by RAFT ([a]Measured by GPC).

Polymer	Structure	Reaction Time (hrs)	Molar % AMA	M_n[a]	M_w[a]	PDI[a]
PO1	POEGMA	24	-	52900	66100	1.25
PA1	POEGMA-*co*-PAMA	24	5	36900	593800	16.11
PA2	POEGMA-*co*-PAMA	12	5	39200	27500	6.90
PA3	POEGMA-*co*-PAMA	24	10	19300	33500	1.73
PA4	POEGMA-*co*-PAMA	12	10	31800	65600	2.06

A low molecular weight distribution (low PDI) – in this case 1.25 – indicates that there is little variation between the chain lengths in the polymer. This is desirable, particularly in biomedical applications, as it means that the properties and behaviour of the resulting polymer are uniform. In a polymeric drug delivery system, for example, a high PDI would result in the different chain lengths being transported and metabolised at different rates. The low polydispersity also indicated that this method was successful in maintaining control over the molecular weight parameters of the polymer synthesised.

^{1}H-NMR was used to analyse the structure of the compound. It is widely accepted that the presence of polymeric groups causes the signals shown on ^{1}H-NMR to broaden (each monomer is similar to its neighbours and therefore the signals overlap) and show less splitting than would be expected for an ^{1}H-NMR spectrum of a monomer or other non-polymeric compounds. It is also common to see multiple peaks for one signal which is indicative of the tacticity of the polymer. Tacticity is the stereochemical arrangement of the units in the main chain of a polymer Chemical shift changes of the different molar constituents of the polymer are caused by differences in the stereochemical environment of the polymer chain[37] - in this case the methylene groups along the polymer backbone are not equivalent due to differing positions of the CH_3 and carbonyl groups. This results in multiple signals as opposed to the single signal which would otherwise be predicted.

In the ^{1}H -NMR spectrum of POEGMA the first signal was observed as three broad singlet peaks at 0.87ppm, 1.03ppm and 1.25ppm. This signal represents the CH_3 protons which are bound to the polymeric back-bone (e-H). The next signal is observed at 1.86ppm which is a quintet, and represents the CH_2 protons in the back-bone of the polymer (d-H). Further downfield, a signal is observed as two singlet peaks at 3.56ppm and 3.66ppm and a triplet at 3.74 ppm. This signal represents the CH_2 protons on the side chain of the polymer (b-H). The final signal is observed at 4.09 ppm which is a singlet peak. This signal represents the CH_2 group on the side chain closest to the ester group on the back-bone of the polymer (c-H). This proximity to the electron withdrawing oxygens on the ester group causes a slight chemical shift to a higher ppm.

End group analysis was not performed due to the absence of a signal corresponding to the aromatic region on the polymer.

Due to server back ups it has not been possible to obtain the exact integrals of the signals at 1.86 ppm and between 1.25 ppm and 0.87 ppm. The spectrum shows that the signal at 1.86 ppm is slightly larger than would be expected for the proton ratios within the signal assignments. GPC results, however, clearly show that a high molecular weight polymer was formed; the reaction mixture became significantly more viscous; and the vinyl peaks have conclusively disappeared. In the weight of

this overwhelming evidence that POEGMA was formed, the difference in integrals was attributed either to an impurity or to starting material left in the polymer after the precipitation.

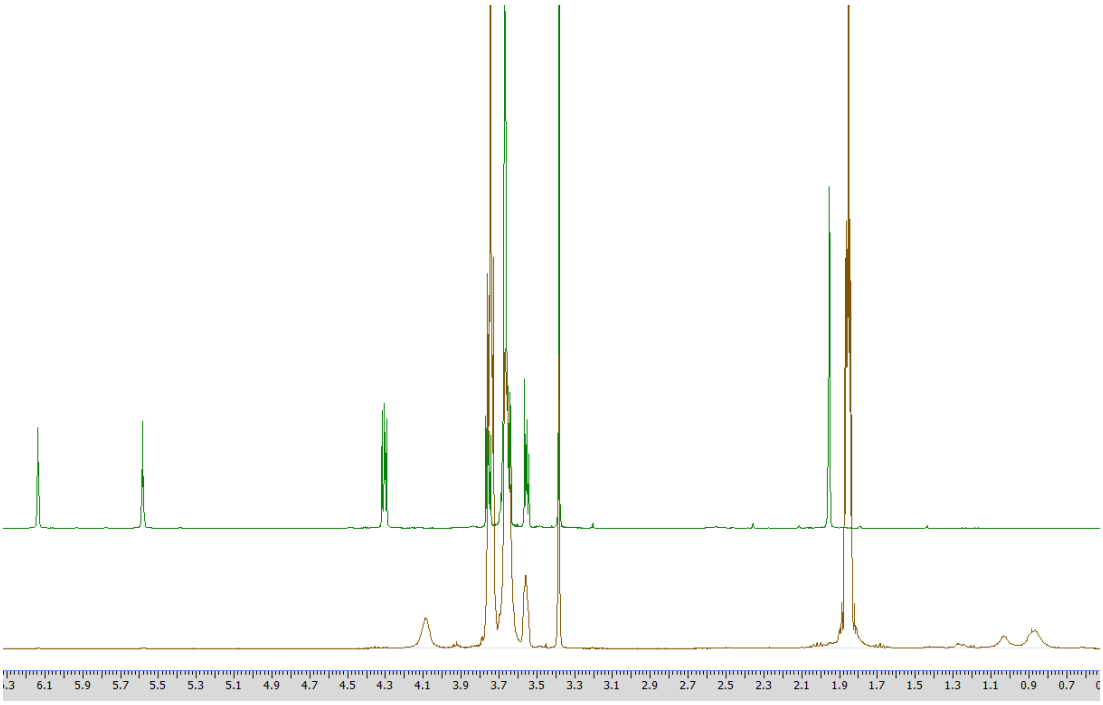

Figure 3.8: Proton NMR Spectra showing the comparison between the OEGMA monomer and POEGMA.

Copolymers of OEGMA with 2-aminoethyl methacrylate (AMA) were also synthesised *via* RAFT polymerisation. The reaction time and the molar percentage of comonomer AMA were varied to investigate the effect on the molecular weight parameters of the resulting polymers. The results of these syntheses are shown in **Table 3.1.**

It is immediately obvious from these results that the addition of a comonomer resulted in increased polydispersity – this could be due to differing reactivity ratios between the two monomers. The polydispersity of 16.11 for PA1 is particularly high, meaning this can no longer be described as a 'living' polymerisation (for which polydispersities must be in the region of 1.5 or below).[25] This reaction was allowed to proceed for 24 hours – in order to determine the level of control over the system, PA1 was repeated but stopped after 12 hours (PA2). This resulted in polymers with

similar average molecular weights to PA1 but a significantly narrower weight distribution. This indicated that towards the end of the reaction, not all chains grow uniformly. In order to prevent this from occurring, components of the RAFT reaction could be systematically varied (for example, changing the temperature or the RAFT agent) to attempt to gain a higher level of control over the polymerisation.

The addition of AMA to the polymeric chain was with a view to binding the copolymer to HYNIC. As such, increasing the proportion of AMA in the copolymer would result in more potential sites at which to bind the HYNIC. This led to the synthesis of PA3 and PA4 (**Table 3.1)**. The increase in AMA molar percentage from 5% to 10% gave polymers of much narrower weight distributions, suggesting the control over polymerisation had improved. For these reactions, however, reducing the time from 24 hours to 12 actually gave polymer chains which were longer than anticipated. This is difficult to explain in terms of polymerisation kinetics, and indicates that a number of other polymerisations would be needed in order to fully understand the system. Varying parameters such as temperature and reaction time could potentially find reaction conditions which maintain the lower polydispersities observed in PA3 and PA4, whilst also giving targeted molecular weights.

As both of the monomers used in the copolymer are methacrylates and therefore have similar structures, the reactivity ratios of the monomers are likely to be comparable. For this reason the polymers obtained during the copolymer are presumed to be random copolymers however further detailed NMR analysis would be necessary to confirm the presence and proportion of AMA in the copolymer.

Although the system has not been optimised in this work, the results demonstrate that RAFT is a viable method of synthesising biocompatible copolymers of OEGMA with AMA.

3.7 Conclusions and Future Work

The aim of this chapter was to synthesise a block copolymer with narrow polydispersity ((M_w/M_n < 1.5) via a RAFT polymerisation technique that could be used to conjugate a HYNIC group. Poly(oligo(ethylene glycol)methacrylate) (POEGMA) was chosen as the back-bone of the copolymer as it is biocompatible. Oligo(ethylene glycol)methacrylates (OEGMAs) are easily polymerisable using reversible addition-fragmentation chain transfer polymerisation (RAFT). The biocompatibility of the oligo(ethylene glycol) (OEG) pendant groups allows POEGMA based materials to be used in the biomedical fields.

POEGMA was synthesised by RAFT and characterised using ^{1}H-NMR spectroscopy. GPC confirmed the polydispersity index of 1.25.

Future work may include the synthesis of POEGMA homopolymers of differing chain lengths, as well as further syntheses of copolymers under varying reaction conditions, such as time and molar percentage of AMA, in order to increase the control over the system. Increasing the molar percentage of AMA may offer narrower polydispersities.

It would be necessary to undertake several reactions under differing conditions and it would be interesting to measure the conversion via NMR which would allow the plotting of kinetic graphs typical of living systems; by combining data about molecular weight with conversion percentages acquired from sampling reactions, standard kinetic plots can be obtained. For living polymerisations these should be linear, which would be a valuable addition to this work, hopefully indicating the 'living' nature of the RAFT polymerisations conducted here.

If the RAFT method was optimised, it would also be useful to synthesise a range of different copolymers to investigate the possible binding sites and efficiency of binding with hydrazine derivatives.

3.8 References

1. J. M. G. Cowie and V. Arrighi, *Polymers: Chemistry and Physics of Modern Materials*, Third Edition edn., CRC Press, 2008.
2. A. Ravve, *Principles of Polymer Chemistry*, Springer, 2012.
3. D. Walton and P. Lorimer, *Polymers*, Oxford University Press, 2000.
4. M. E. Aulton and K. M. G. Taylor, *Aulton's Pharmaceutics: The Design and Manufacture of Medicines*, Elsevier Health Sciences UK, 2013.
5. R. J. Young and P. A. Lovell, *Introduction to Polymers, Third Edition*, Taylor & Francis, 2011.
6. in *Encyclopedia of Polymer Science and Technology*, John Wiley & Sons, Inc., 2002.
7. O. Parisi, M. Curcio and F. Puoci, in *Advanced Polymers in Medicine*, ed. F. Puoci, Springer International Publishing, 2015, pp. 1-31.
8. C. Hagiopol, *Copolymerization: Toward a Systematic Approach*, Kluwer/Plenum, 1999.
9. B. Sitharaman, *Nanobiomaterials Handbook*, CRC Press, 2011.
10. U. Gedde, *Polymer Physics*, Springer, 1995.
11. E. Saldivar-Guerra and E. Vivaldo-Lima, *Handbook of Polymer Synthesis, Characterization, and Processing*, Wiley, 2013.
12. A. Noshay and J. E. McGrath, *Block Copolymers: Overview and Critical Survey*, Elsevier Science, 2013.
13. F. H. Schacher, P. A. Rupar and I. Manners, *Angewandte Chemie International Edition*, 2012, **51**, 7898-7921.
14. J. E. McGrath, *Journal of Chemical Education*, 1981, **58**, 914.
15. in *Statistical, Gradient, Block and Graft Copolymers by Controlled/Living Radical Polymerizations*, Springer Berlin Heidelberg, 2002, vol. 159, pp. 14-29.
16. D. B. Millward and S. E. Sills, *Methods of forming block copolymers*, US 20120046415 A1, 2012.
17. P. Bahadur, *Current Science Bangalore*, 2001, **80**, 1002-1007.
18. A.-V. Ruzette and L. Leibler, *Nature materials*, 2005, **4**, 19-31.

19. G. Odian, *Principles of Polymerization*, Wiley, 2004.
20. V. Mishra and R. Kumar, *Journal of Scientific Research, BHU, Varanasi*, 2012, **56**, 141-176.
21. G. Moad, J. Chiefari, R. T. A. Mayadunne, C. L. Moad, A. Postma, E. Rizzardo and S. H. Thang, *Macromolecular Symposia*, 2002, **182**, 65-80.
22. P. Bahadur, 2001.
23. G. Moad, J. Chiefari, J. Krstina, R. T. A. Mayadunne, A. Postma, E. Rizzardo and S. H. Thang, *Polymer International*, 2000, **49**, 993-1001.
24. J. Chiefari, Y. K. Chong, F. Ercole, J. Krstina, J. Jeffery, T. P. T. Le, R. T. A. Mayadunne, G. F. Meijs, C. L. Moad, G. Moad, E. Rizzardo and S. H. Thang, *Macromolecules*, 1998, **31**, 5559-5562.
25. R. P. Quirk and B. Lee, *Polymer International*, 1992, **27**, 359-367.
26. W. A. Braunecker and K. Matyjaszewski, *Progress in Polymer Science*, 2007, **32**, 93-146.
27. J. Chiefari, Y. Chong, F. Ercole, J. Krstina, J. Jeffery, T. P. Le, R. T. Mayadunne, G. F. Meijs, C. L. Moad and G. Moad, *Macromolecules*, 1998, **31**, 5559-5562.
28. B. Trzebicka, D. Szweda, S. Rangelov, A. Kowalczuk, B. Mendrek, A. Utrata-Wesolek and A. Dworak, *Journal of Polymer Science Part a-Polymer Chemistry*, 2013, **51**, 614-623.
29. G. Moad, E. Rizzardo and S. H. Thang, *Accounts of Chemical Research*, 2008, **41**, 1133-1142.
30. G. Moad, J. Chiefari, Y. K. Chong, J. Krstina, R. T. A. Mayadunne, A. Postma, E. Rizzardo and S. H. Thang, *Polymer International*, 2000, **49**, 993-1001.
31. J.-F. Lutz, O. Akdemir and A. Hoth, *Journal of the American Chemical Society*, 2006, **128**, 13046-13047.
32. J. F. Lutz, *Journal of Polymer Science Part a-Polymer Chemistry*, 2008, **46**, 3459-3470.
33. M. Allmeroth, D. Moderegger, B. Biesalski, K. Koynov, F. Rosch, O. Thews and R. Zentel, *Biomacromolecules*, 2011, **12**, 2841-2849.
34. M. Hruby, J. Kucka, M. Novakova, H. Mackova and M. Vetrik, *Applied Radiation and Isotopes*, 2010, **68**, 334-339.

35. S. W. Prescott, M. J. Ballard, E. Rizzardo and R. G. Gilbert, *Macromolecules*, 2002, **35**, 5417-5425.
36. J. F. Quinn, E. Rizzardo and T. P. Davis, *Chemical Communications*, 2001, 1044-1045.
37. C. K. Ober, *Journal of Chemical Education*, 1989, **66**, 645.

Chapter 4 - Conclusions and Future Work

4.1 Conclusions

This thesis presents the synthesis of various HYNIC analogues that are capable of chelating technetium-99m in order to be attached to an amino acid and incorporated into a peptide sequence via solid phase peptide synthesis (SPPS) to image site-specific targets. While 6-HYNIC has been widely used, 2-HYNIC has not, and as such both of these were used in the synthesis of a number of derivatives.

These derivatives were characterised by ^{1}H and ^{13}C NMR, FT-IR and melting point data was obtained for comparison with literature. Two different HYNIC analogues (2-HYNIC and 6-HYNIC) and their BOC-protected forms were successfully synthesised in high yields with the aim of binding these to copolymer chains. The syntheses of these compounds are non-trivial and required multiple attempts and several changes to the literature methods. Preliminary experiments were performed, and ^{1}H-NMR and ^{13}C-NMR spectra for these reactions have shown to be either unsuccessful or inconclusive, demonstrating the limitations of the approach for synthesising HYNIC and its analogues.

6-HYNIC has been synthesised according to a modified prep in 74% yield. 6-Boc-HYNIC has been synthesised according to a modified prep in 98% yield. NHS-HYNIC-BOC has been synthesised according to a modified prep in 98% yield. 2-HYNIC has been synthesised according to a modified prep in 51% yield. 2-Boc-HYNIC has been synthesised according to a modified prep in 86% yield.

This work also presents the synthesis of a bifunctional copolymer (POEGMA-co-PAMA) which is biocompatible and can be attached to a HYNIC group and subsequently a peptide. This copolymer was synthesised using a controlled living radical polymerisation technique called Reversible Addition Fragmentation chain Transfer (RAFT). This technique was chosen due to its ability to synthesise polymers with predetermined molecular weights of complex architectures whilst maintaining control over polydispersity. Copolymers of varying compositions were synthesised and analysed by GPC and NMR. Poly(oligo(ethylene

glycol)methacrylate) (POEGMA) was chosen as the back-bone of the copolymer as it is biocompatible. POEGMA was synthesised by RAFT and characterised using ^{1}H-NMR spectroscopy. GPC confirmed the polydispersity index of 1.25.

4.2 Future Work

2-HYNIC provides and possible promising alternative to 6-HYNIC as a BFC for binding with technetium-99m. It would be useful to determine whether 2-HYNIC gives analogous results to 6-HYNIC and furthermore if 2-HYNIC offers a better profile for some radiopharmaceuticals. As 2-HYNIC has been used very little in the literature, a number of different coligands could be explored in order to improve the hydrophilicity and stability of the technetium complex with 2-HYNIC.

In addition, the RAFT method requires optimisation. The optimised method would allow for the copolymer to be labelled with technetium-99m for SPECT, providing an alternative bioconjugate synthetic route.

Future work may also include the synthesis of POEGMA homopolymers of differing chain lengths, as well as further syntheses of copolymers under varying reaction conditions, such as time and molar percentage of AMA, in order to increase the control over the system. Increasing the molar percentage of AMA may offer narrower polydispersities.

It would be necessary to undertake several reactions under differing conditions and it would be interesting to measure the conversion via NMR which would allow the plotting of kinetic graphs typical of living systems; by combining data about molecular weight with conversion percentages acquired from sampling reactions, standard kinetic plots can be obtained. For living polymerisations these should be linear, which would be a valuable addition to this work, hopefully indicating the 'living' nature of the RAFT polymerisations conducted here.